

# **Special Topics Reservoir Simulation Report**

**June 2018 to May 2019**

## TABLE OF CONTENTS

1 Data collection	4
1.1 Initial reservoir simulation model	4
2 History matching of waterflooding	6
2.1 Layer cake model	6
2.2 Heterogeneous model	10
2.3 Permeability strip model	15
3 History matching of polymer flooding	17
3.1 Change of well constraint	18
3.2 History matching results	19
4 Tracer test data for history matching	27
4.1 Parameter setting of the reservoir simulation model	28
4.2 History matching results	29
4.3 Updated reservoir simulation model	33
5 Reservoir EOR performance prediction	34
6 Conclusions	37
7 Future work	38

## LIST OF FIGURES

Figure 1: The initial relative permeability curves of (a) oil/water and (b) gas/oil	5
Figure 2: The grid top diagram of the initial reservoir simulation model	6
Figure 3: Layer cake model demonstrated by permeability distribution	7
Figure 4: Oil production rates of (a) producer J27 and (b) producer J28	8
Figure 5: History matching results of (a) gas production rate (b) water cut for producer J27 and (c) gas production rate (d) water cut for producer J28	10
Figure 6: Heterogeneity of (a) permeability and (b) porosity distribution	11
Figure 7: History matching results of (a) gas production rate (b) water cut for producer J27 and (c) gas production rate (d) water cut for producer J28	14
Figure 8: The estimated relative permeability curves of (a) oil/water and (b) gas/oil	15
Figure 9: Permeability strips in the reservoir simulation model	15
Figure 10: History matching results of (a) gas production rate (b) water cut for producer J27 and (c) gas production rate (d) water cut for producer J28	17
Figure 11: Actual and simulated well bottom hole pressures of (a) producer J27 and (b) producer J28	18
Figure 12: Permeability heterogeneity of (a) 8-strips, (b) 16-strips, (c) 32-strips, and (d) 16-blocks	21
Figure 13: History matching results of producer J27 water cut for four cases	23
Figure 14: History matching results of well bottom hole pressure for (a) producer J27 and (b) producer J28	24
Figure 15: A new set of relative permeability curves of (a) oil/water and (b) gas/oil	25
Figure 16: History matching results of (a) water cut (b) oil production rate for producer J27 and (c) water cut (d) oil production rate for producer J28	27
Figure 17: Permeability heterogeneity of block/strip type in the simulation model	28
Figure 18: History matching results of (a) water cut (b) oil production rate for producer J27 and (c) water cut (d) oil production rate for producer J28	31

Figure 19: History matching results of (a) T140A concentration (b) T140C concentration in producer J27 and (c) T140A concentration (d) T140C concentration in producer J28	33
Figure 20: Updated permeability heterogeneity of the reservoir simulation model	33
Figure 21: Predicted production profiles of (a) water cut (b) oil production rate in producer J27 and (c) water cut (d) oil production rate in producer J28	36
Figure 22: The profiles of oil recovery factor of the entire field by injecting different amounts of polymer in the next 10 years	37

### LIST OF TABLES

Table 1: Average values of porosity and permeability for five layers	4
Table 2: Coefficients of the power-law model in the history matching process	12

### Nomenclature

3D	Three Dimensional
$a_g$	Maximum of Gas Phase Relative Permeability (Equation 3)
$a_o$	Maximum of Oil Phase Relative Permeability (Equation 2 and 4)
$a_w$	Maximum of Water Phase Relative Permeability (Equation 1)
bbl	Barrel
bhp	Bottomhole Pressure
EOR	Enhanced Oil Recovery
HM	History Matching
$k_{rg}$	Relative Permeability of Gas in a Two Phase Gas-Oil System
$k_{rog}$	Relative Permeability of Oil in a Two Phase Gas-Oil System
$k_{row}$	Relative Permeability of Oil in a Two Phase Oil-Water System
$k_{rw}$	Relative Permeability of Water in a Two Phase Oil-Water System
$k_x/k_y/k_y$	Directional Permeability
md or mD	MilliDarcy
$n_g$	Corey Exponent of Gas
$n_{og}$	Corey Exponent of Oil in a Two Phase Gas-Oil System
$n_{ow}$	Corey Exponent of Oil in a Two Phase Water-Oil System
$n_w$	Corey Exponent of Water
LPR	Liquid Production Rate
OPR	Oil Production Rate
PPB	Parts Per Billion
SC	Standard Conditions
SF	Skin Factor
$S_g$	Gas Saturation
$S_{gc}$	Critical Gas Saturation
$S_{or}$	Residual Oil Saturation
$S_{org}$	Residual Oil Saturation to Gas
$S_{orw}$	Residual Oil Saturation to Water
$S_w$	Water Saturation
$S_{wi}$	Irreducible Water Saturation

From June 2018 to May 2019, UAF built the reservoir simulation model using data provided by Hilcorp Alaska. Then the history matching of waterflooding and polymer flooding was conducted, respectively. During the history matching process, the permeability heterogeneity and relative permeability were primarily tuned to obtain the optimal reservoir simulation model. Finally, the production performance of waterflooding and polymer flooding was forecasted, respectively, using the updated reservoir simulation model, and their results were compared.

**1 Data collection**

The following fluid properties, rock-fluid interaction data, and production data have been provided by Hilcorp Alaska:

- $k_x/k_y$  and  $k_x/k_z$
- reference reservoir pressure for fluid properties
- water properties: compressibility, viscosity, formation volume factor, salinity
- oil properties
- oil-water, oil-gas relative permeability and capillary pressure curves
- rock compressibility
- initial reservoir pressure and initial oil and water saturation
- well perforations data
- radii for injection wells and production wells

All these data are classified as Limited Rights Data since they have been collected and interpreted using the operator’s private funding. Government and recipients must obtain written permission from Hilcorp Alaska, LLC prior to disclosure or use of these Limited Rights Data.

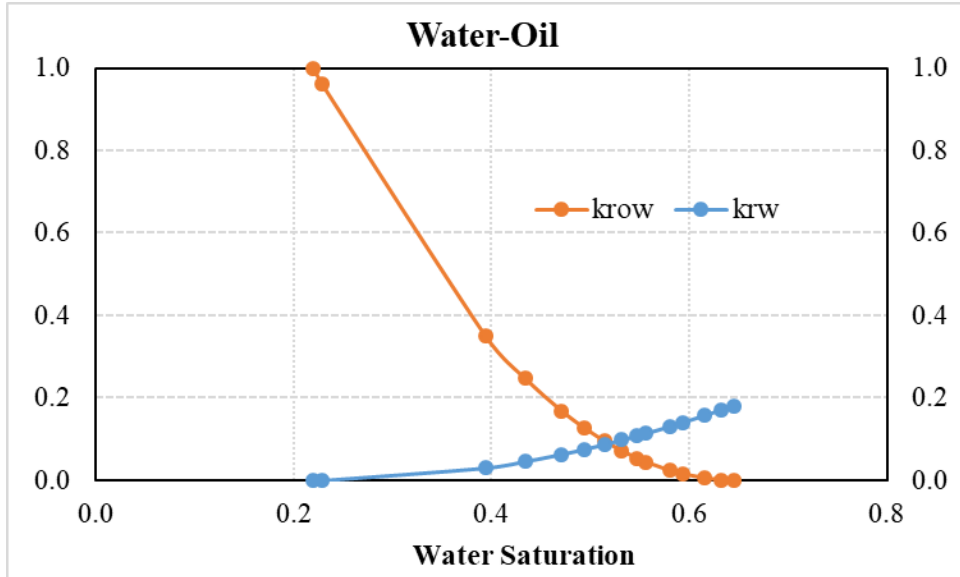
**1.1 Initial reservoir simulation model**

The three-dimensional (3D) grid system of the initial reservoir simulation model has been generated based on the geological model provided by Hilcorp geologist. In the reservoir simulation model, the number of total blocks is 51,480, including 18,651 active blocks. The average values of porosity and permeability for five layers are presented in **Table 1**.

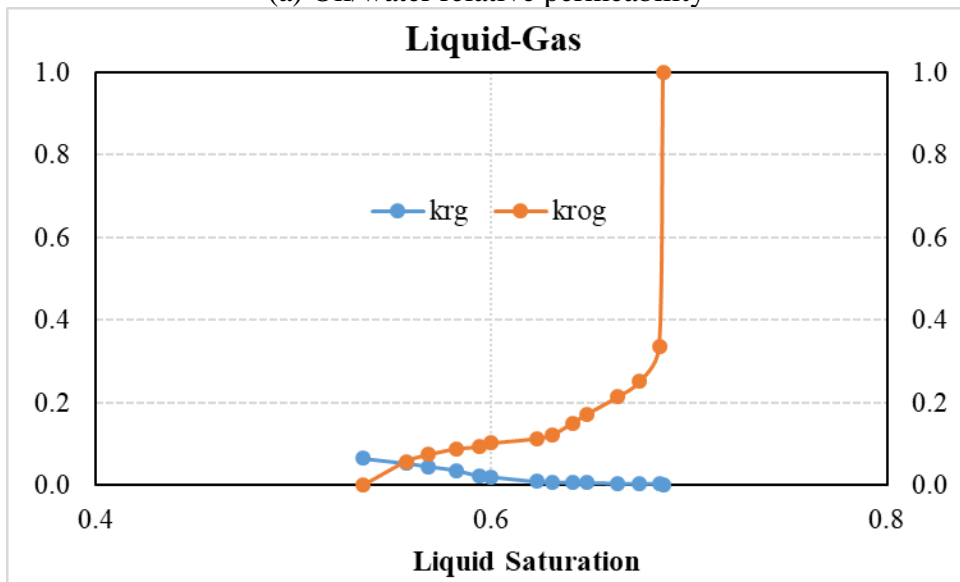
**Table 1: Average values of porosity and permeability for five layers**

	Layer 1	Layer 2	Layer 3	Layer 4	Layer 5
Porosity	0.3476	0.3474	0.3537	0.3497	0.3417
Permeability (mD)	1806	1598	2269	1801	1029

The initial relative permeability curves of oil/water and gas/oil are shown in **Figure 1**. By integrating the aforementioned data, the initial reservoir simulation model is established, as shown in **Figure 2**, which illustrates the formation, faults, and horizontal well distribution.



(a) Oil/water relative permeability



(b) Gas/oil relative permeability

**Figure 1: The initial relative permeability curves of (a) oil/water and (b) gas/oil**

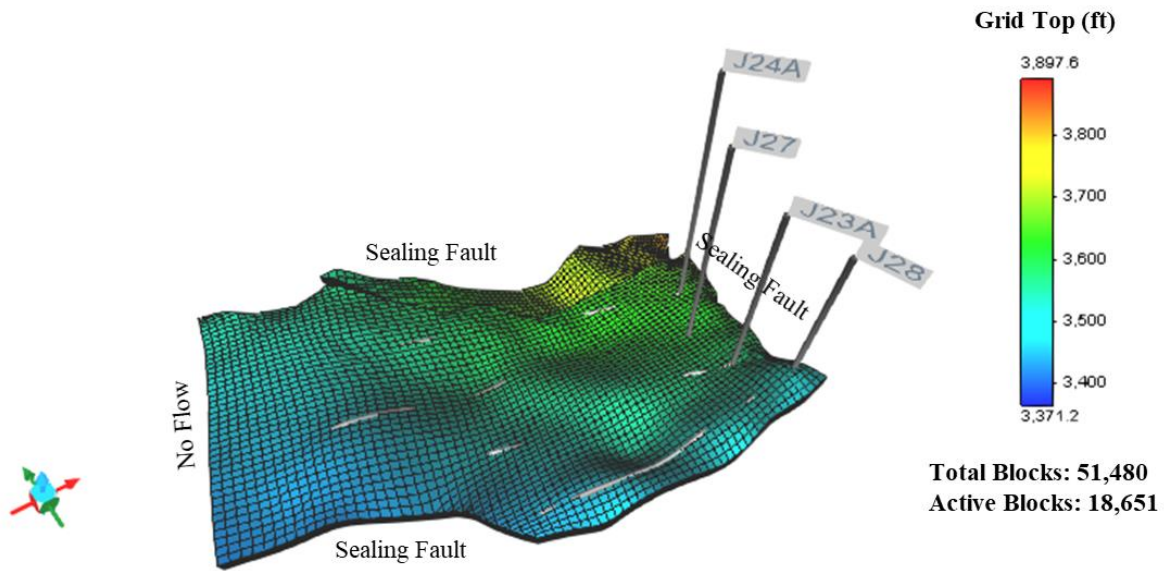


**Figure 2: The grid top diagram of the initial reservoir simulation model**

## 2 History matching of waterflooding

CMOST, a module of the CMG simulator, is used to conduct the history matching with the assistance of advanced algorithms. Since water injection rate and oil production rate are used as well constraints in the reservoir simulation model, only water cut and gas production rate of two production wells need to be matched in the history matching process. The permeability and the relative permeability curves are modified step by step to match the waterflooding production history. First, the homogeneous permeability in each layer is tuned in a layer cake model. Second, the relative permeability curves are tuned in a heterogeneous model. Finally, the permeability distribution in a strip manner is tuned with the estimated relative permeability curves.

### 2.1 Layer cake model

The layer cake model is shown in **Figure 3**. The permeability in each layer is homogeneous and initially assigned with the corresponding average permeability. In addition, the porosity of each layer is fixed at its average value. In the history matching process, only the homogeneous permeability in each layer is tuned varying from 100 to 7600 mD, which is in line with the core data.

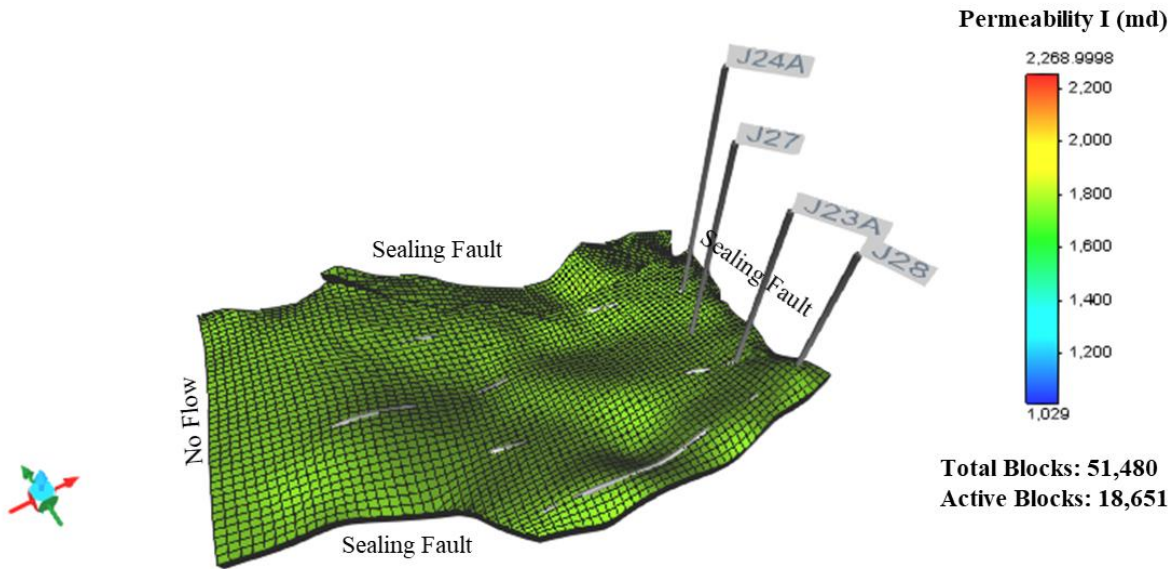
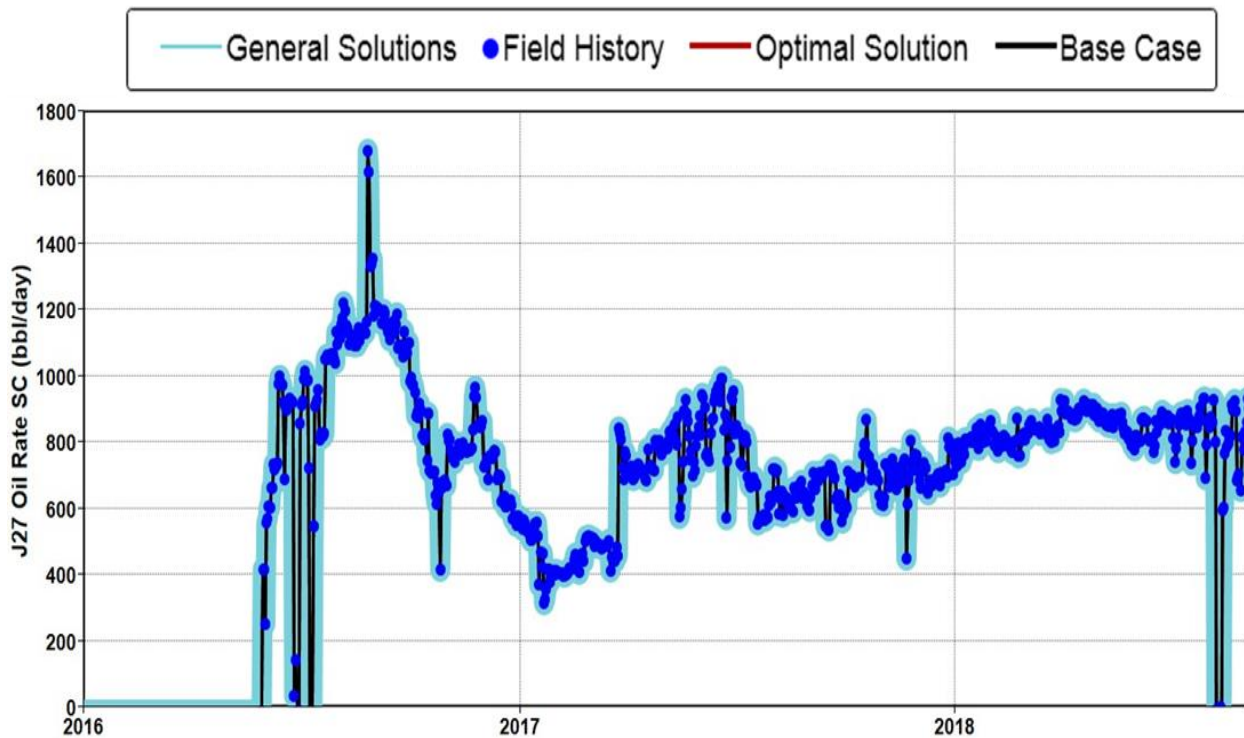
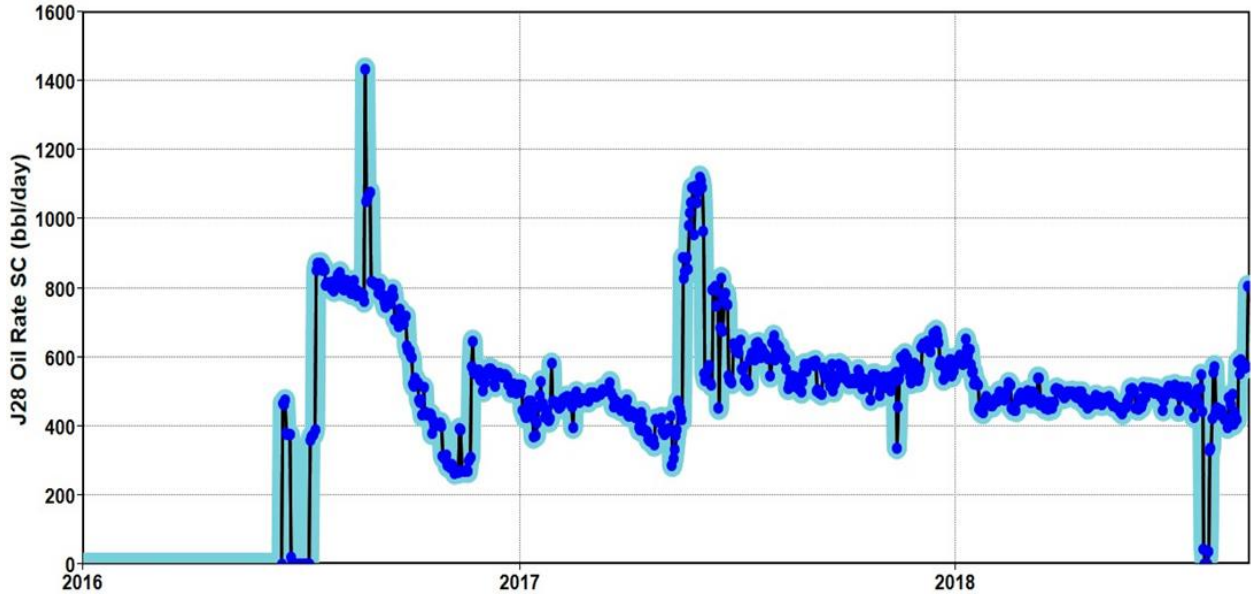


**Figure 3: Layer cake model demonstrated by permeability distribution**

Oil production rates, as well constraints, in the simulation model are presented in **Figure 4**, which correspond to the actual ones. The history matching results of water cut and gas production rate for two production wells are shown in **Figure 5**. The dots are actual field data and the black line represents the initial production response in the simulation model prior to the history matching. The red line is the production response of the best-matched simulation model.

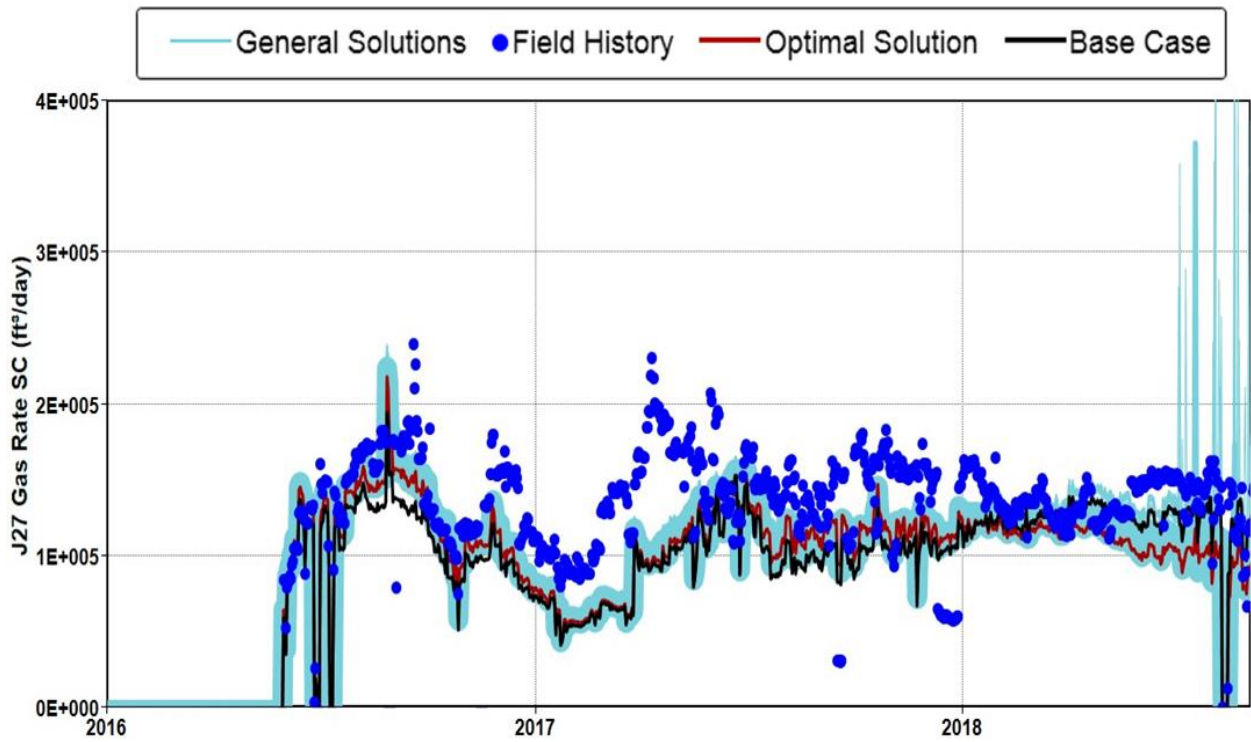


(a) Oil production rate of producer J27



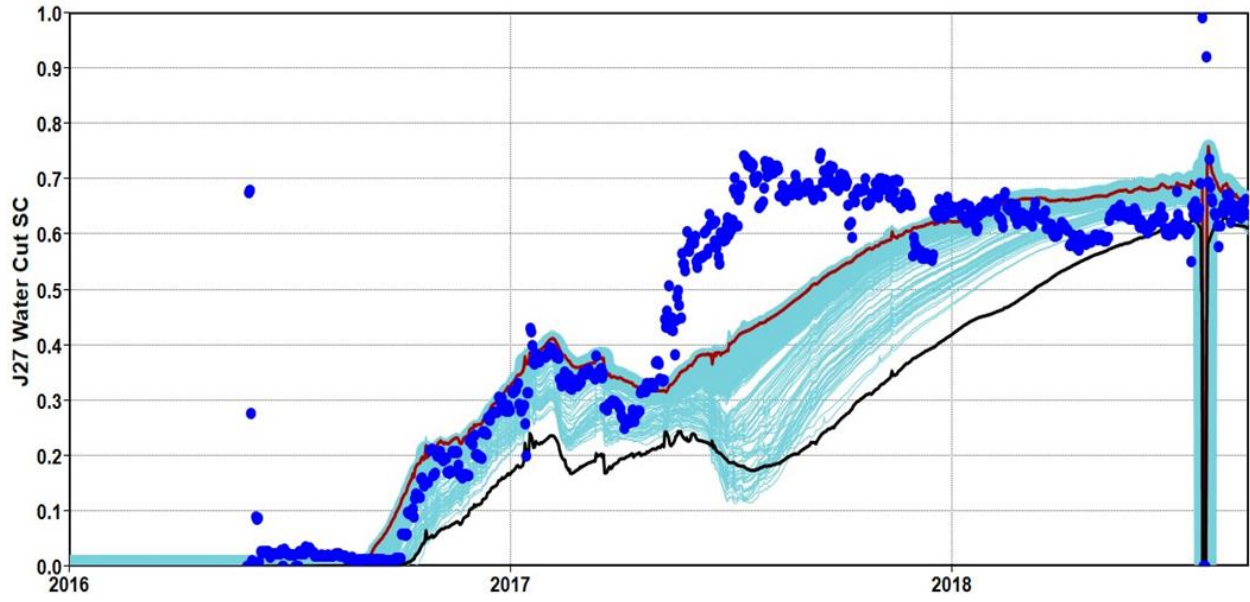
(b) Oil production rate of producer J28

Figure 4: Oil production rates of (a) producer J27 and (b) producer J28

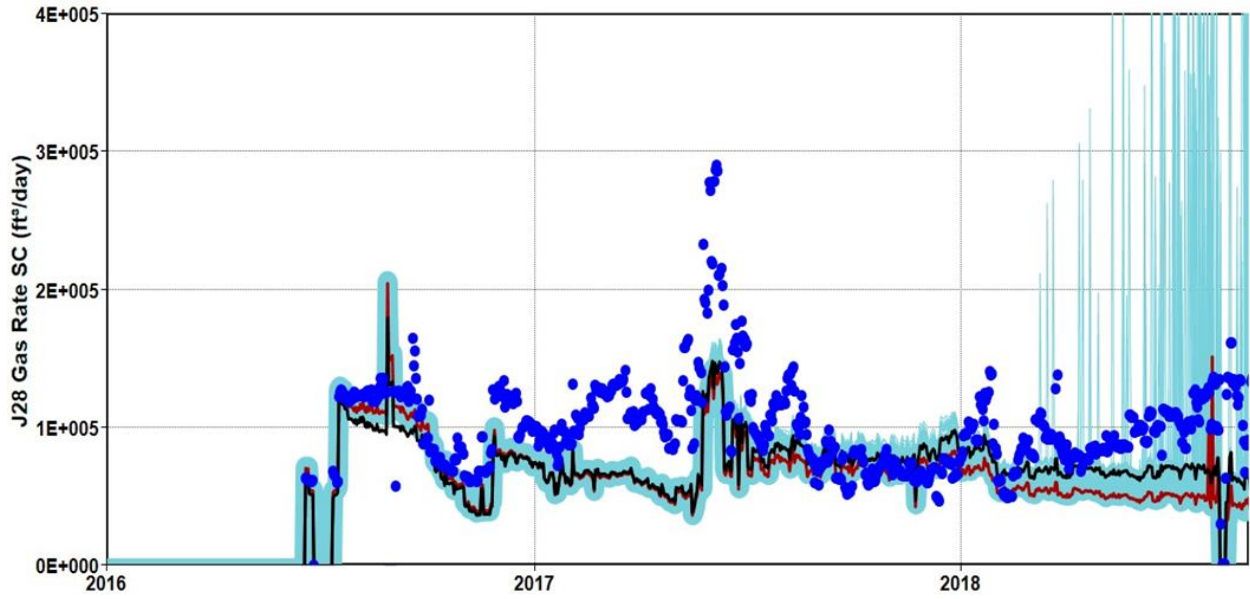


(a) Gas production rate of producer J27

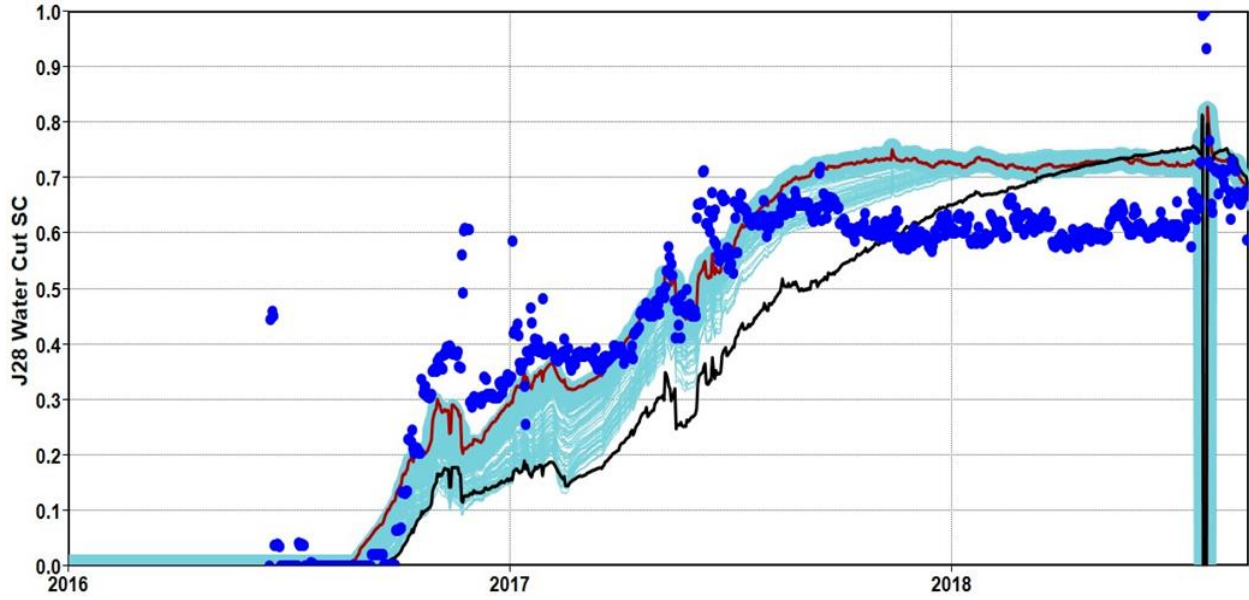




(b) Water cut of producer J27



(c) Gas production rate of producer J28



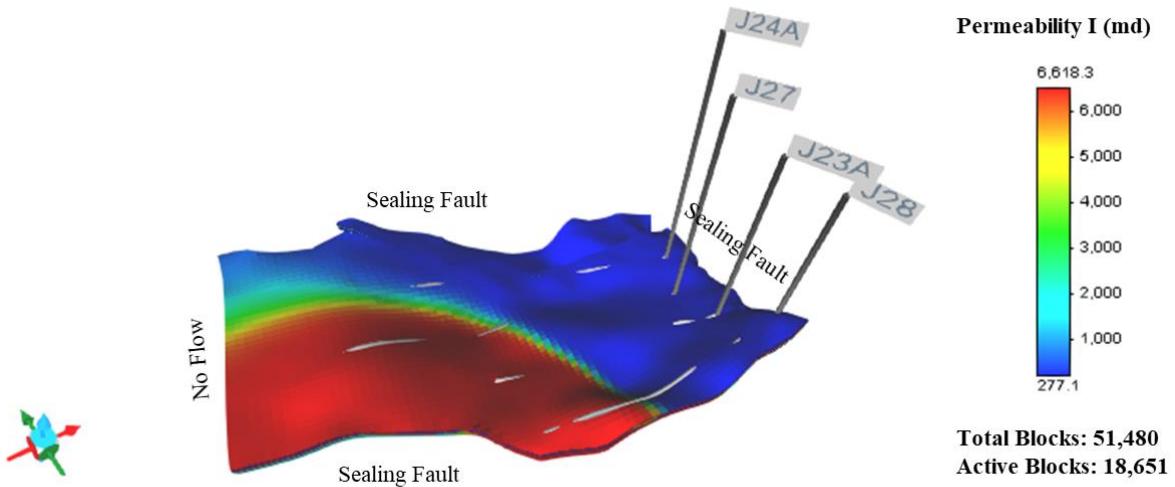
(d) Water cut of producer J28

**Figure 5: History matching results of (a) gas production rate (b) water cut for producer J27 and (c) gas production rate (d) water cut for producer J28**

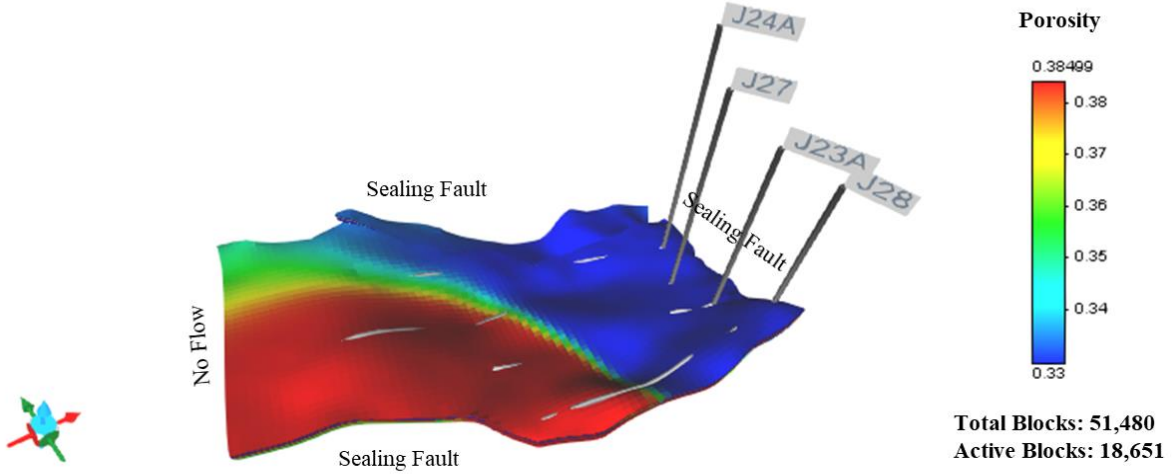
It has been found that using homogeneous permeability in each layer cannot reproduce the water cut curves with humps. To improve the history matching results, the permeability and porosity arrays provided by the geological model are used in the heterogeneous model.

## 2.2 Heterogeneous model

The heterogeneity of permeability and porosity distribution are shown in **Figure 6**.



(a) Heterogeneity of permeability distribution



(b) Heterogeneity of porosity distribution

**Figure 6: Heterogeneity of (a) permeability and (b) porosity distribution**

In this case, the relative permeability curves are tuned to match the waterflooding production history. First, the relative permeability is parameterized by using the power-law model. For the oil-water system, the relative permeability is represented by:

$$k_{rw}(S_w) = a_w \left( \frac{S_w - S_{wi}}{1 - S_{wi} - S_{orw}} \right)^{n_w} \quad (1)$$

$$k_{row}(S_w) = a_o \left( \frac{1 - S_w - S_{orw}}{1 - S_{wi} - S_{orw}} \right)^{n_{ow}} \quad (2)$$

where  $k_{rw}(S_w)$  and  $k_{row}(S_w)$  are the water and oil phase relative permeability, respectively;  $a_w$  and  $a_o$  are the maximum of water and oil phase relative permeability, respectively;  $S_w$  is water saturation;  $S_{wi}$  is irreducible water saturation;  $S_{orw}$  is residual oil saturation (to water);  $n_w$  and  $n_{ow}$  are the exponents controlling the curvatures of relative permeability curves.

As for the oil-gas system, the relative permeability is similarly expressed by:

$$k_{rg}(S_g) = a_g \left( \frac{S_g - S_{gc}}{1 - S_{wi} - S_{gc} - S_{org}} \right)^{n_g} \quad (3)$$

$$k_{rog}(S_g) = a_o \left( \frac{1 - S_{wi} - S_g - S_{org}}{1 - S_{wi} - S_{gc} - S_{org}} \right)^{n_{og}} \quad (4)$$

where  $k_{rg}(S_g)$  and  $k_{rog}(S_g)$  are the gas and oil phase relative permeability, respectively;  $a_g$  is the maximum of gas phase relative permeability;  $S_g$  is gas saturation;  $S_{gc}$  is critical gas saturation;  $S_{org}$

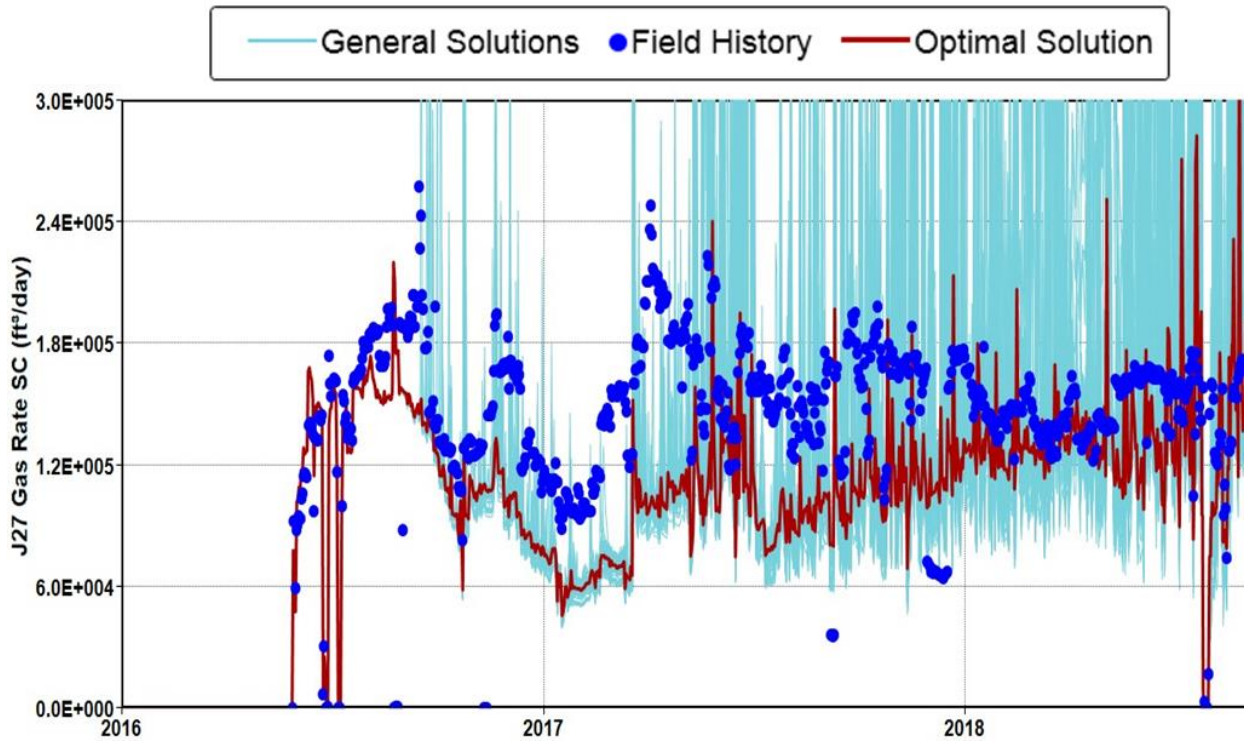
is residual oil saturation (to gas);  $n_g$  and  $n_{og}$  are the exponents controlling the curvatures of relative permeability curves.

Based on laboratory measured core data,  $a_o$  and  $S_{wi}$  are set as 1.0 and 0.235, respectively. The other coefficients of the power-law model are directly tuned in the history matching process. The initial value, adjustment range and the estimated value of these coefficients are described in **Table 2**.

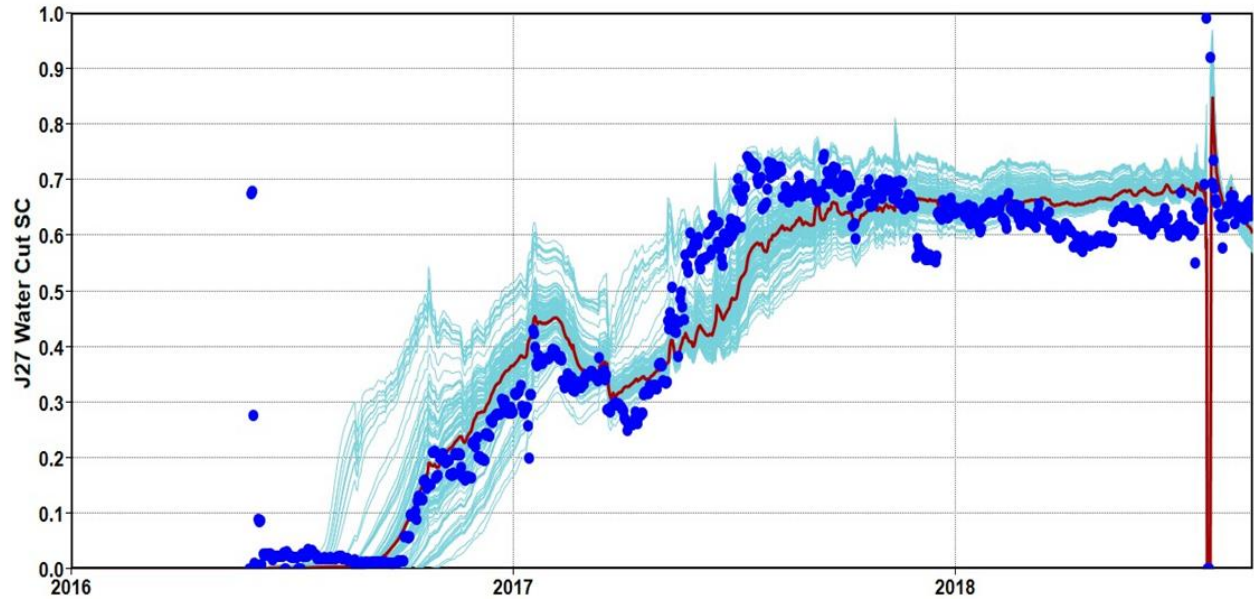
**Table 2: Coefficients of the power-law model in the history matching process**

Variable	Initial Value	Range	Estimated Value
$S_{orw}$	0.32	0.30-0.35	0.31
$a_w$	0.35	0.15-0.50	0.33
$n_w$	2.00	1.00-4.00	1.50
$n_{ow}$	2.00	1.50-4.00	2.70
$S_{org}$	0.20	0.10-0.30	0.20
$S_{gc}$	0.02	0.01-0.06	0.02
$a_g$	0.30	0.10-1.00	1.00
$n_{og}$	2.00	1.50-3.50	1.69
$n_g$	2.00	1.50-4.50	2.10

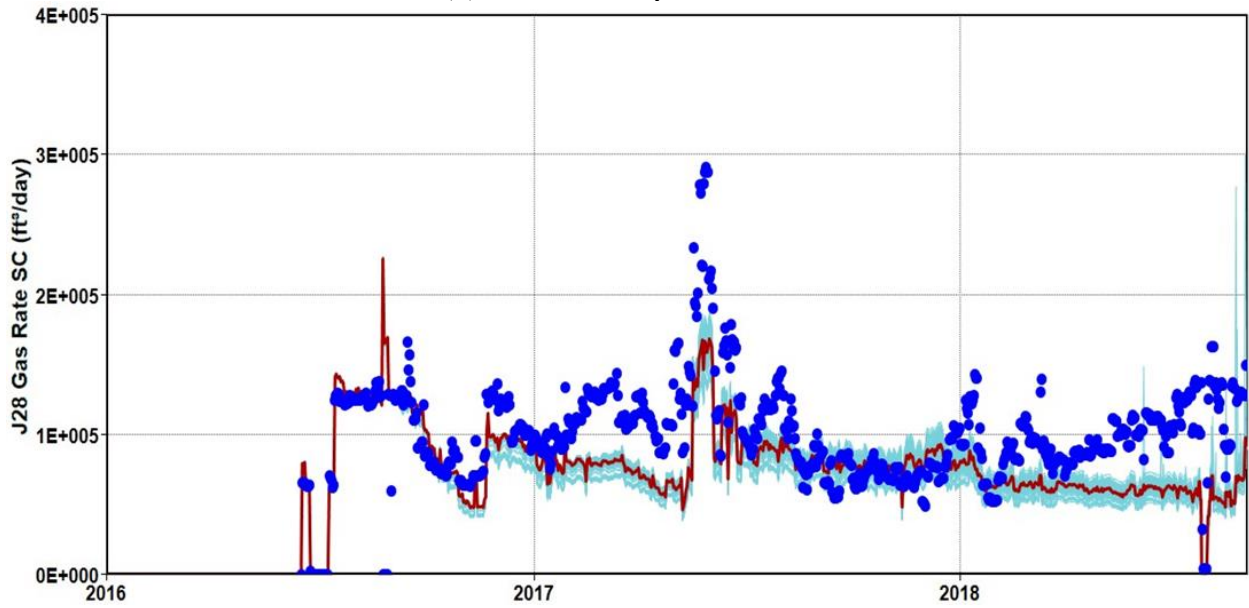
It is worth noting that the actual oil production rates are well reproduced in the simulation model. The history matching results by optimizing the coefficients of the power-law model are shown in **Figure7**.



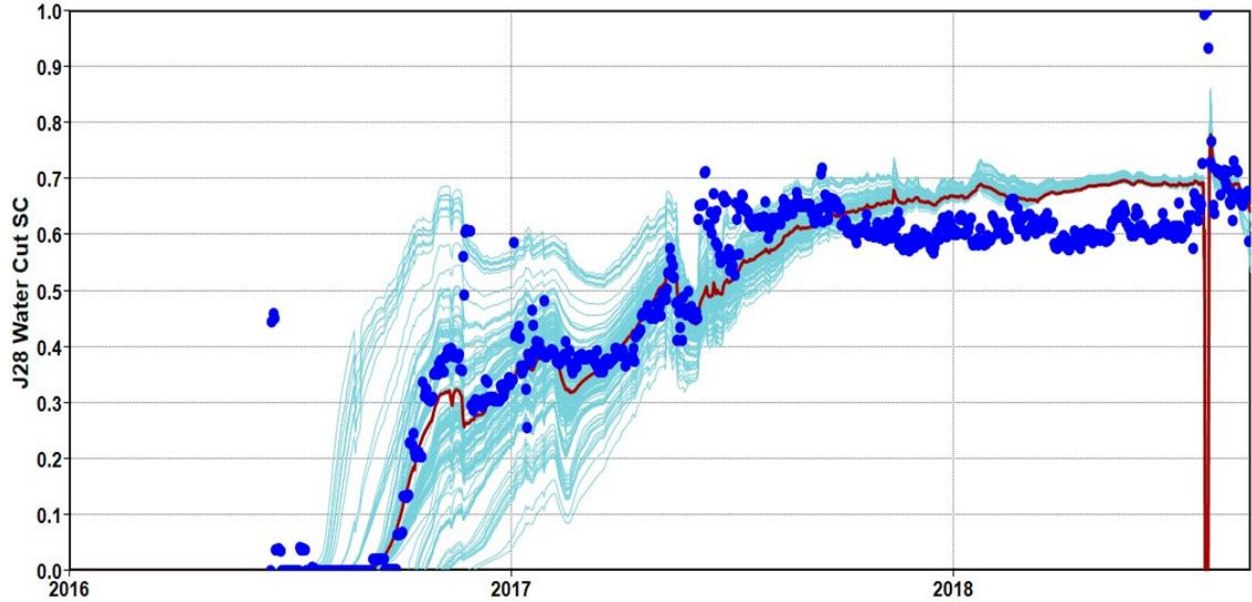
(a) Gas production rate of producer J27



(b) Water cut of producer J27



(c) Gas production rate of producer J28

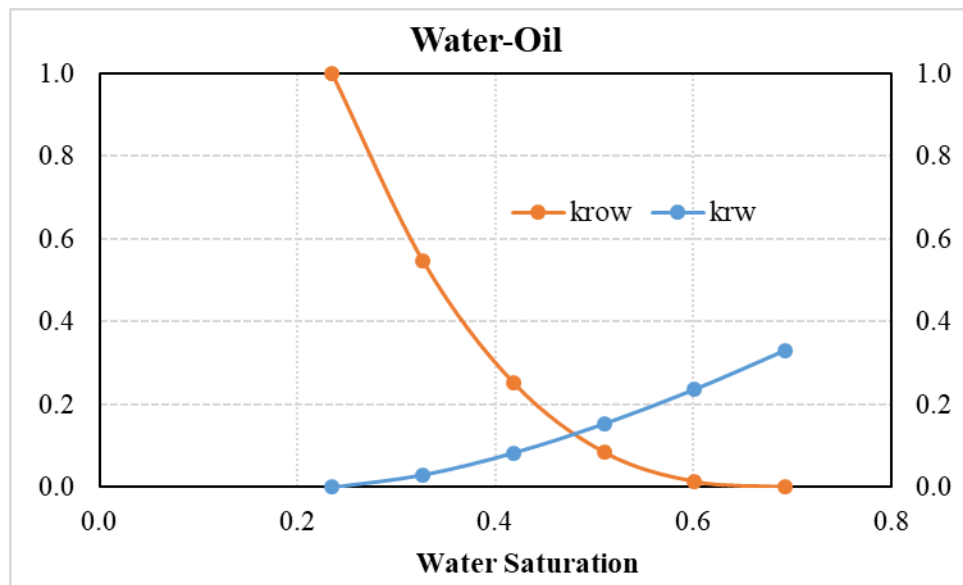


(d) Water cut of producer J28

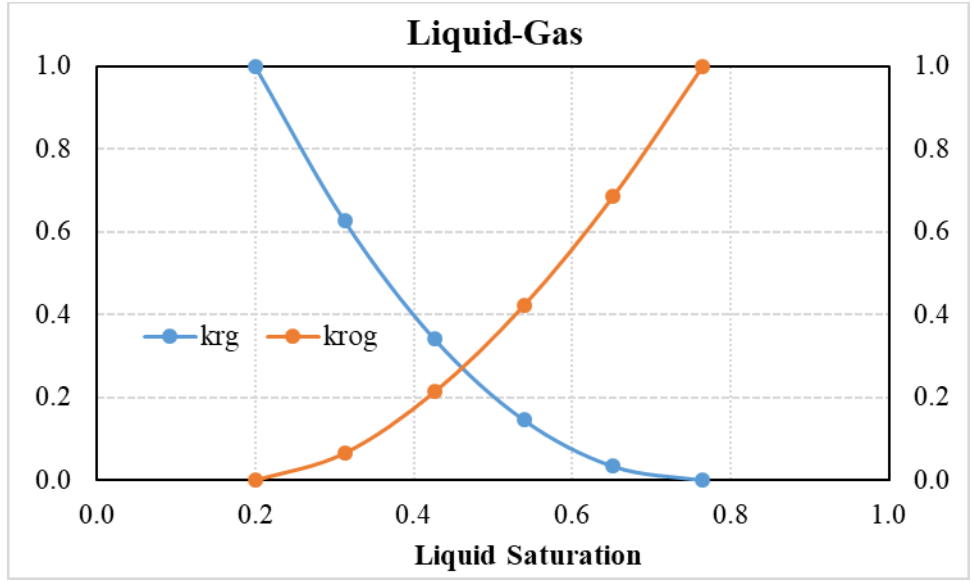
**Figure 7: History matching results of (a) gas production rate (b) water cut for producer J27 and (c) gas production rate (d) water cut for producer J28**

As can be seen, a close agreement can be found between the simulated and the actual water cut curves for both production wells. In other words, the estimated relative permeability curves are able to capture the multiphase flow performance to a large extent in the waterflooding process.

Given the estimated coefficients of the power-law model, the updated water-oil and oil-gas relative permeability curves can be plotted, as shown in **Figure 8**.



(a) Oil/water relative permeability



(b) Gas/oil relative permeability

**Figure 8: The estimated relative permeability curves of (a) oil/water and (b) gas/oil**

**2.3 Permeability strip model**

A permeability strip model is developed, as shown in **Figure 9**, to further investigate the heterogeneity of the field pilot reservoir. Nine permeability strips are assigned in each layer, resulting in 45 permeability strips in the reservoir simulation model. The permeabilities of the strips in each layer are initially assigned with the average permeability of the layer and then tuned between 100 and 7600 mD during the history matching process. In addition, the average porosity of each layer is used and the updated relative permeability curves, as shown in **Figure 8**, are also used in the simulation model.

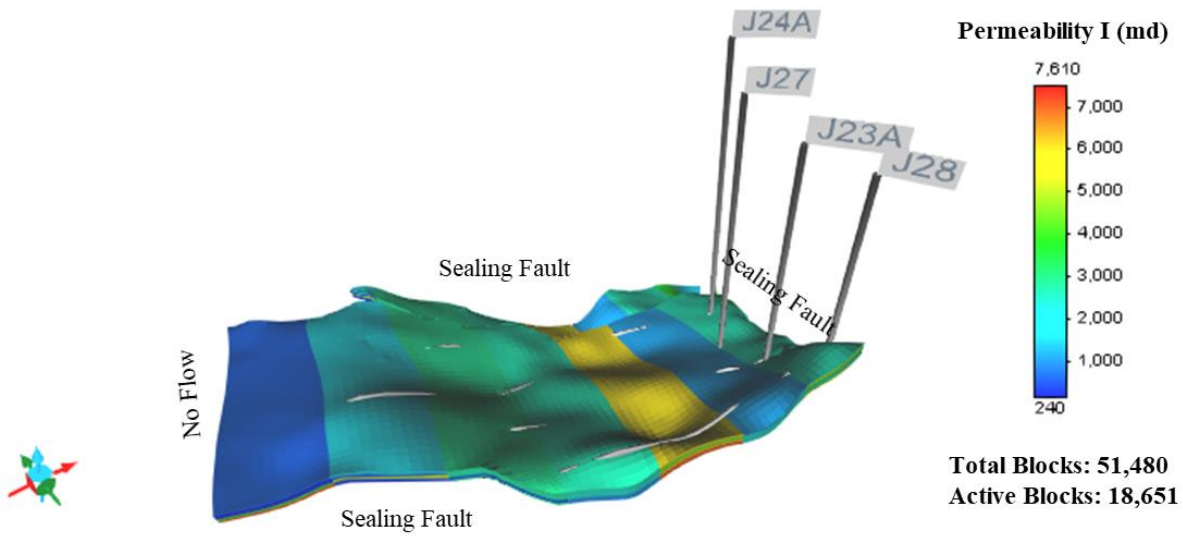
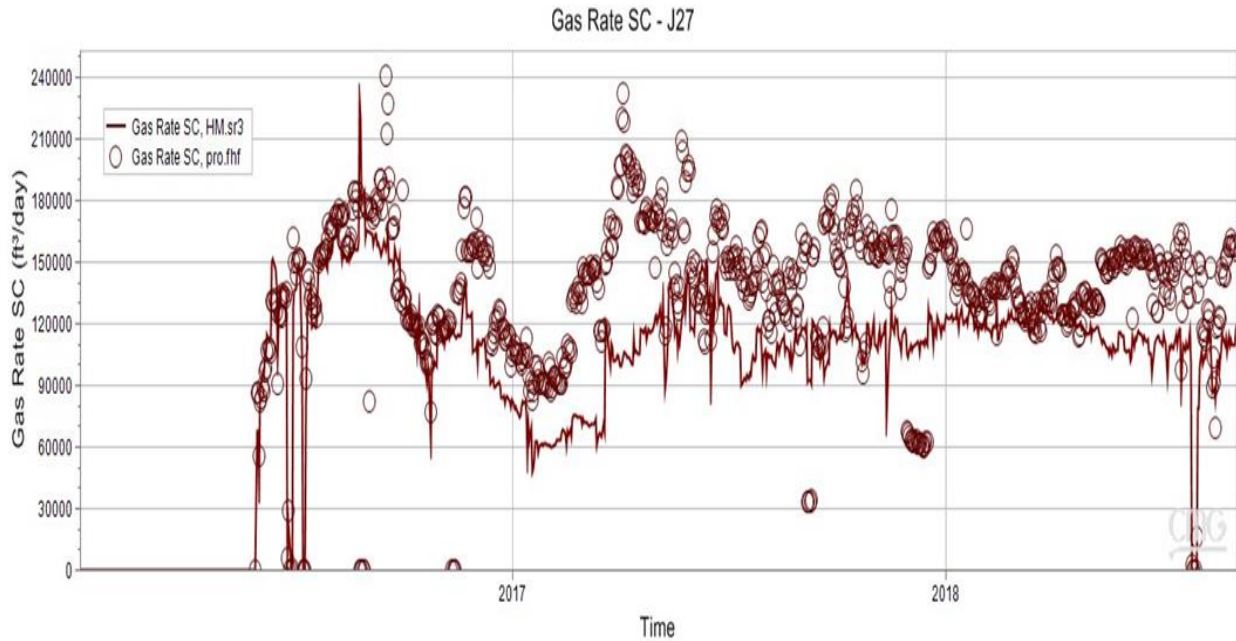
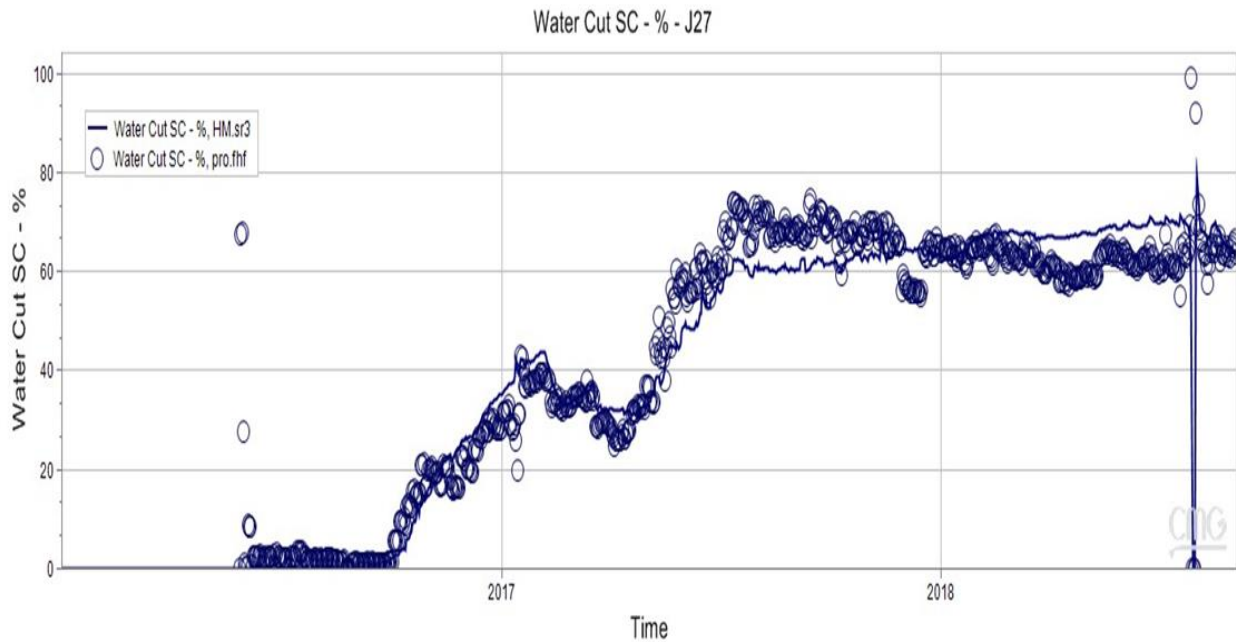


**Figure 9: Permeability strips in the reservoir simulation model**

The actual oil production rates are also reproduced in the simulation model. The optimal history matching results in the permeability strip models are shown in **Figure 10**. The humps on the water cut curves have been well reproduced in the simulation due to the heterogeneous and strip type permeability distribution.

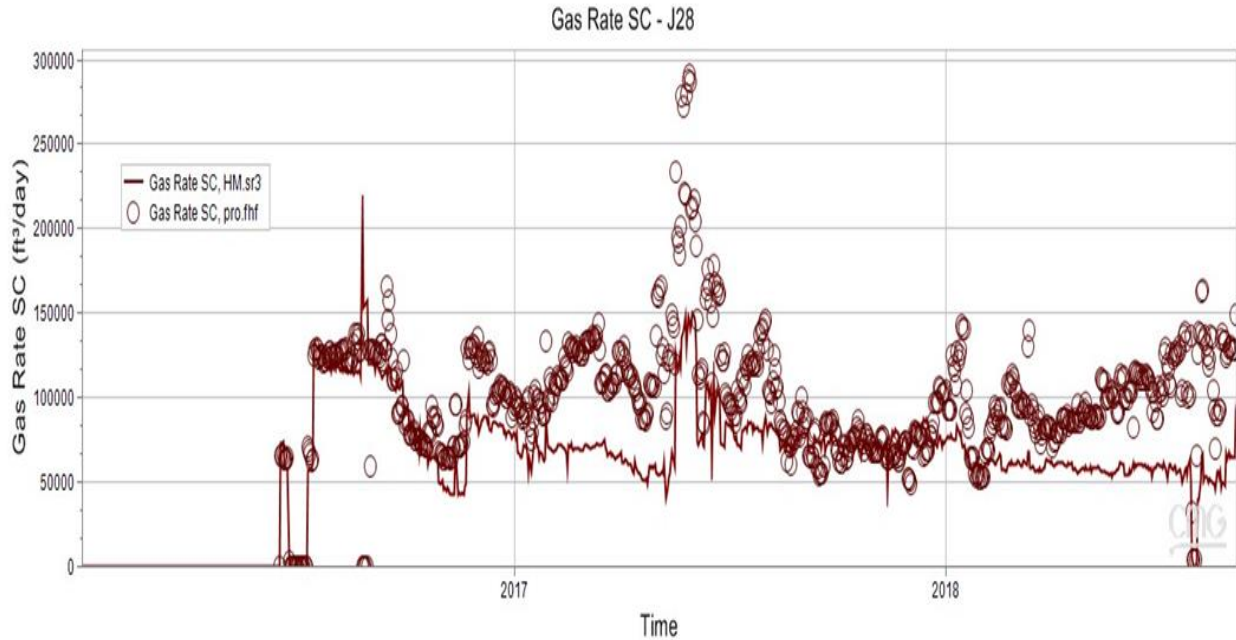


(a) Gas production rate of producer J27

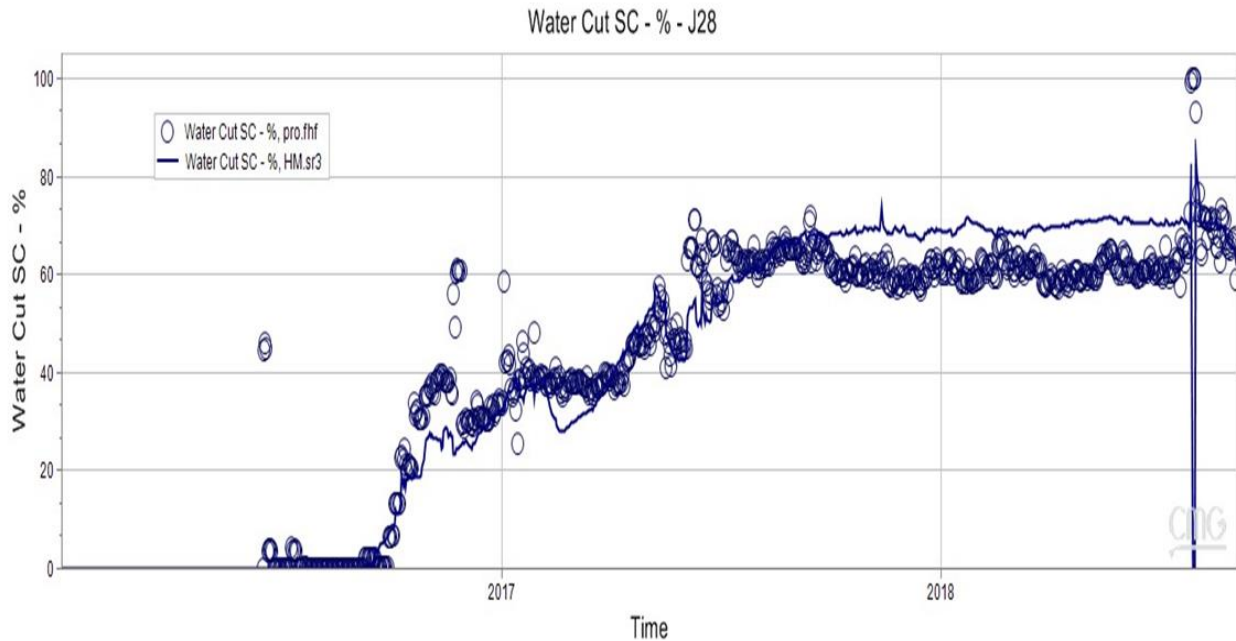


(b) Water cut of producer J27





(c) Gas production rate of producer J28



(d) Water cut of producer J28

**Figure 10: History matching results of (a) gas production rate (b) water cut for producer J27 and (c) gas production rate (d) water cut for producer J28**

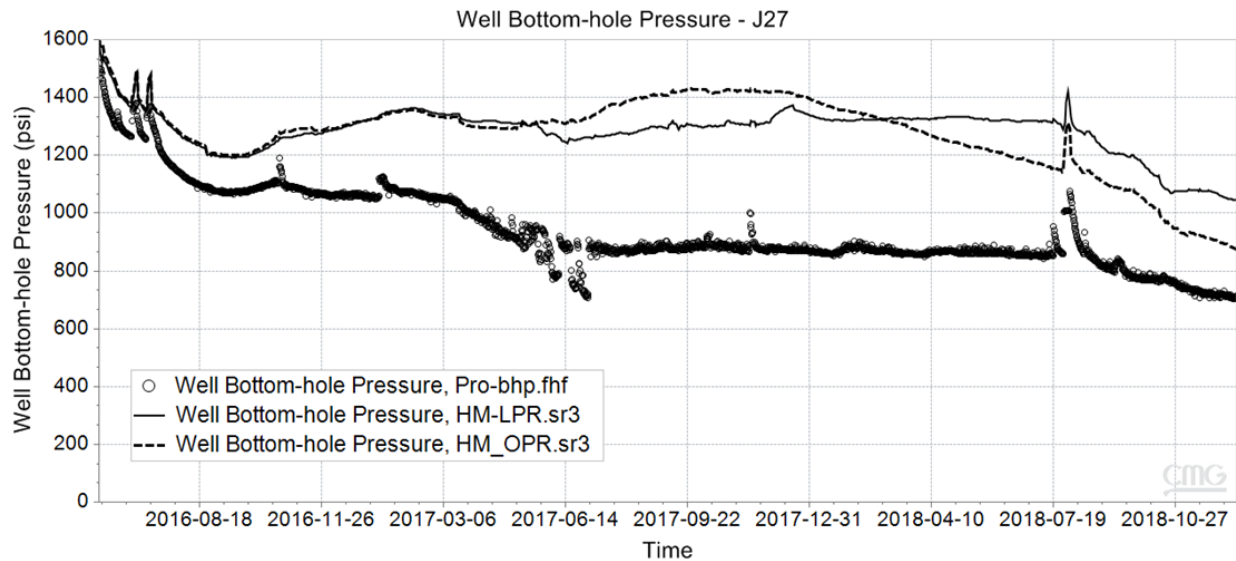
### 3 History matching of polymer flooding

By collecting production data from the polymer injection, the production history used to tune the reservoir simulation model is extended to December 16, 2018. The well constraints including well injection rates and oil, water and gas production rates have been renewed in the reservoir

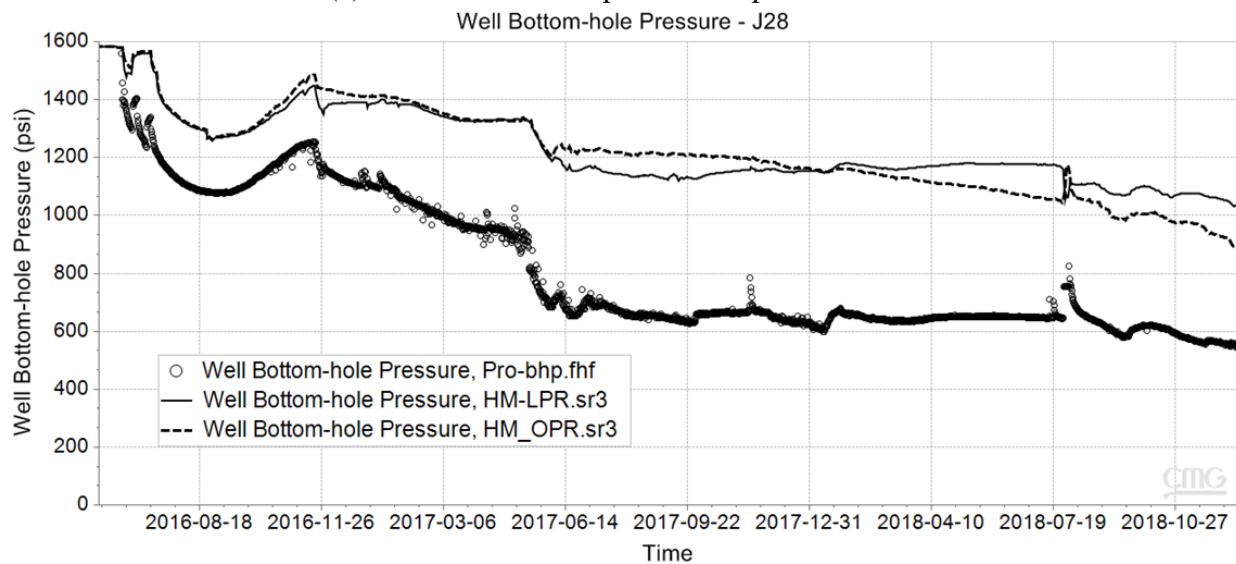
simulation model. Besides, the well bottom hole pressure of two production wells is used to calibrate the reservoir simulation model.

### 3.1 Change of well constraint

Given the extended production data, we try to match not only the production profiles of waterflooding and polymer flooding but also the well bottom hole pressure of two production wells. In order to investigate which well constraints can be used to get a more realistic well bottom hole pressure, the well bottom hole pressures obtained by using oil production rate (OPR) and liquid production rate (LPR) as well constraints respectively, are shown in **Figure 11**. The dots are actual field data. The solid line and dash line represent the simulated well bottom hole pressure using the oil production rate and liquid production rate as well constraint, respectively.



(a) Well bottom hole pressure of producer J27



(b) Well bottom hole pressure of producer J28

**Figure 11: Actual and simulated well bottom hole pressures of (a) producer J27 and (b) producer J28**

It is found that the results of using oil production rate as well constraint cannot capture the actual trend of the well bottom hole pressure. Therefore, the liquid production rate is employed as the new well constraint in the reservoir simulation model.

### 3.2 History matching results

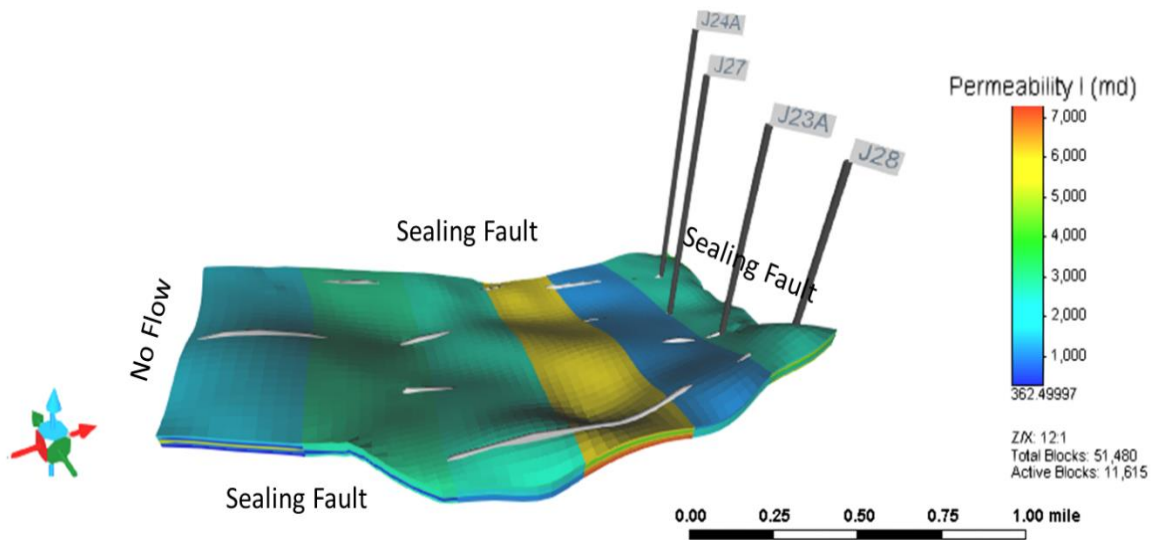
**Permeability Heterogeneity.** The permeability heterogeneity is varied to match the production profiles and well bottom hole pressure simultaneously. The following four cases represent the permeability heterogeneity, as shown in **Figure 12**.

Case #1: 8 strips in each layer, 40 parameters to be tuned in total

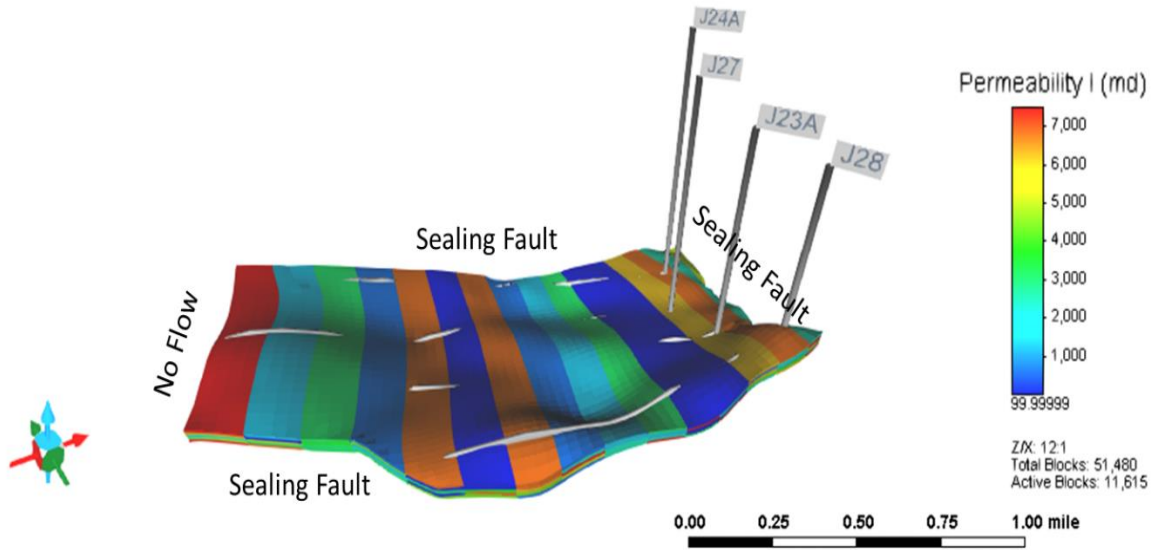
Case #2: 16 strips in each layer, 80 parameters to be tuned in total

Case #3: 32 strips in each layer, 160 parameters to be tuned in total

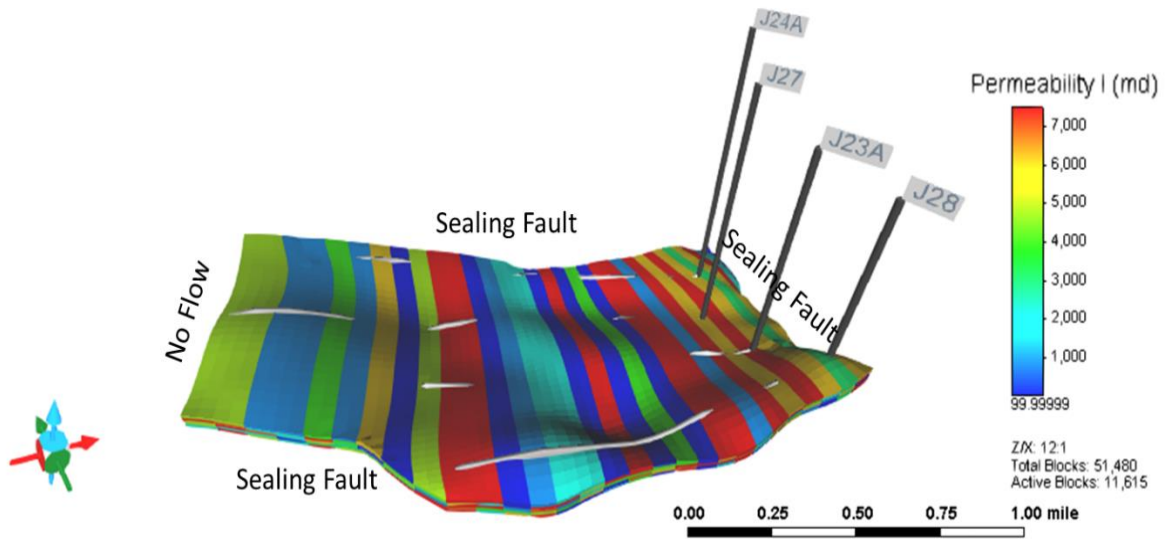
Case #4: 16 blocks in each layer, 80 parameters to be tuned in total



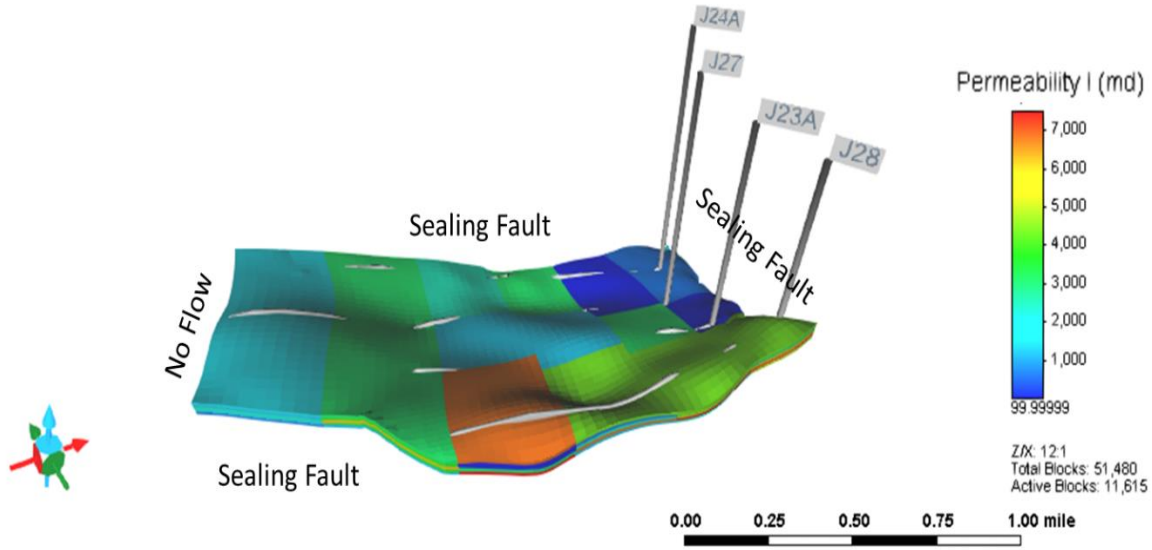
(a) Permeability heterogeneity of 8 strips (Case #1)



(b) Permeability heterogeneity of 16 strips (Case #2)



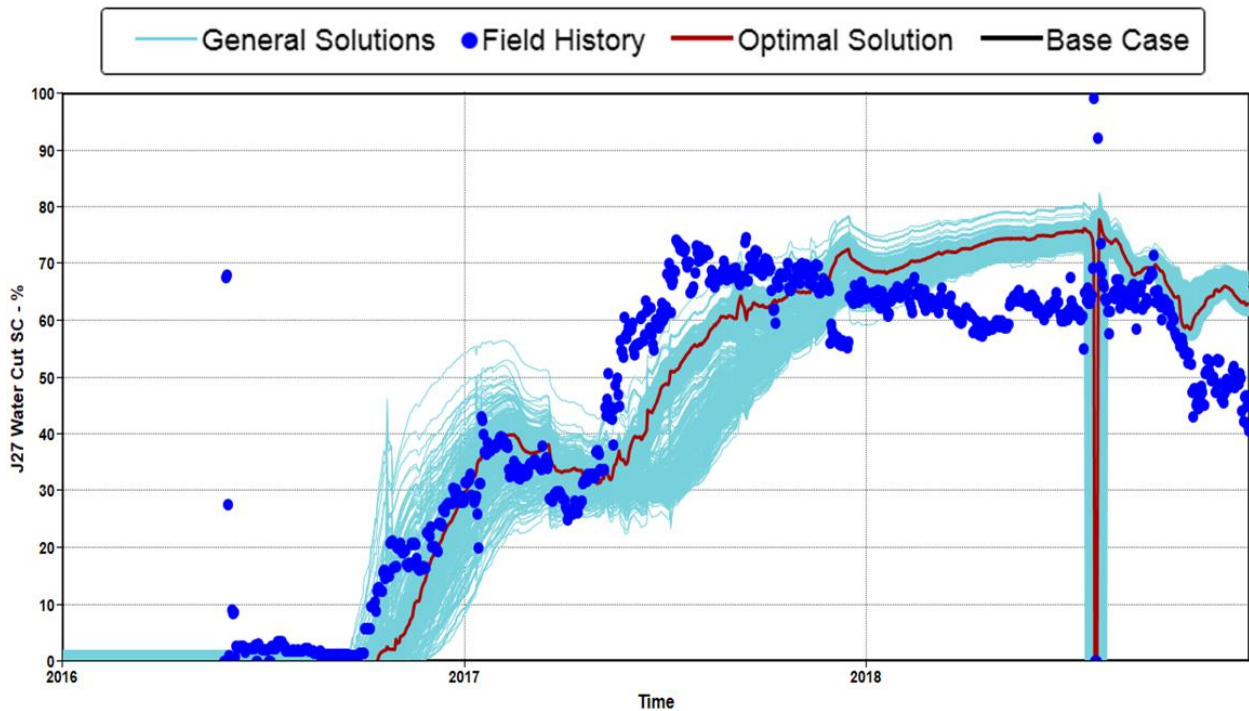
(c) Permeability heterogeneity of 32 strips (Case #3)



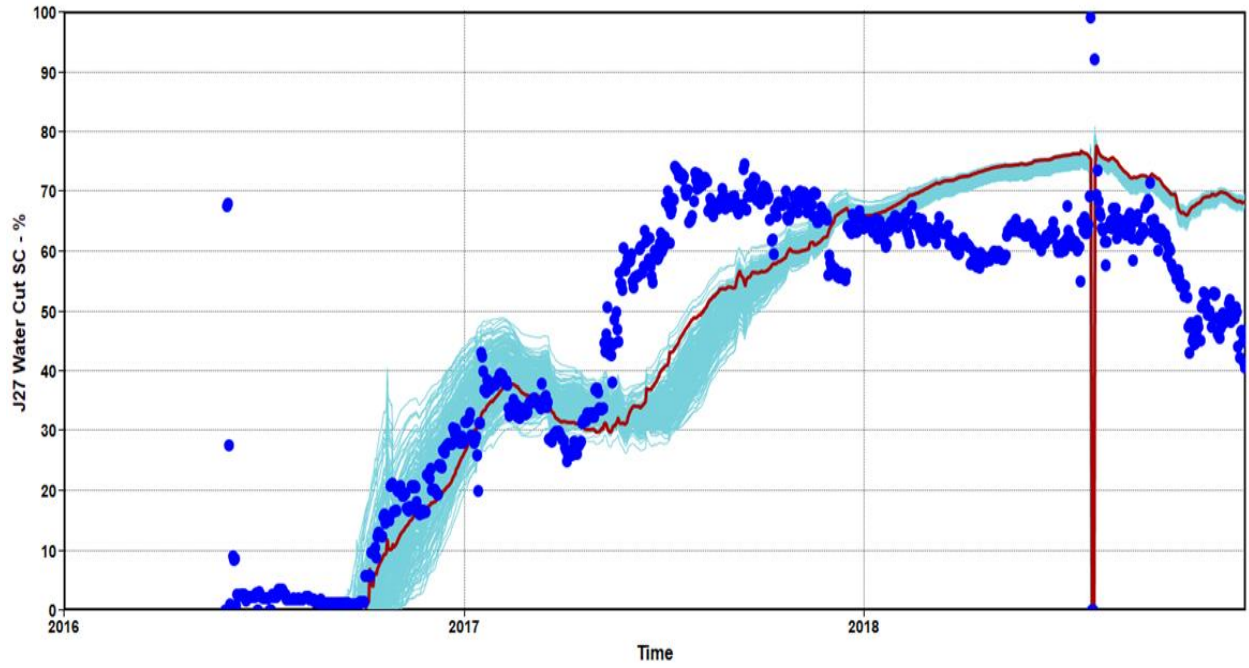
(d) Permeability heterogeneity of 16 blocks (Case #4)

**Figure 12: Permeability heterogeneity of (a) 8-strips, (b) 16-strips, (c) 32-strips, and (d) 16-blocks**

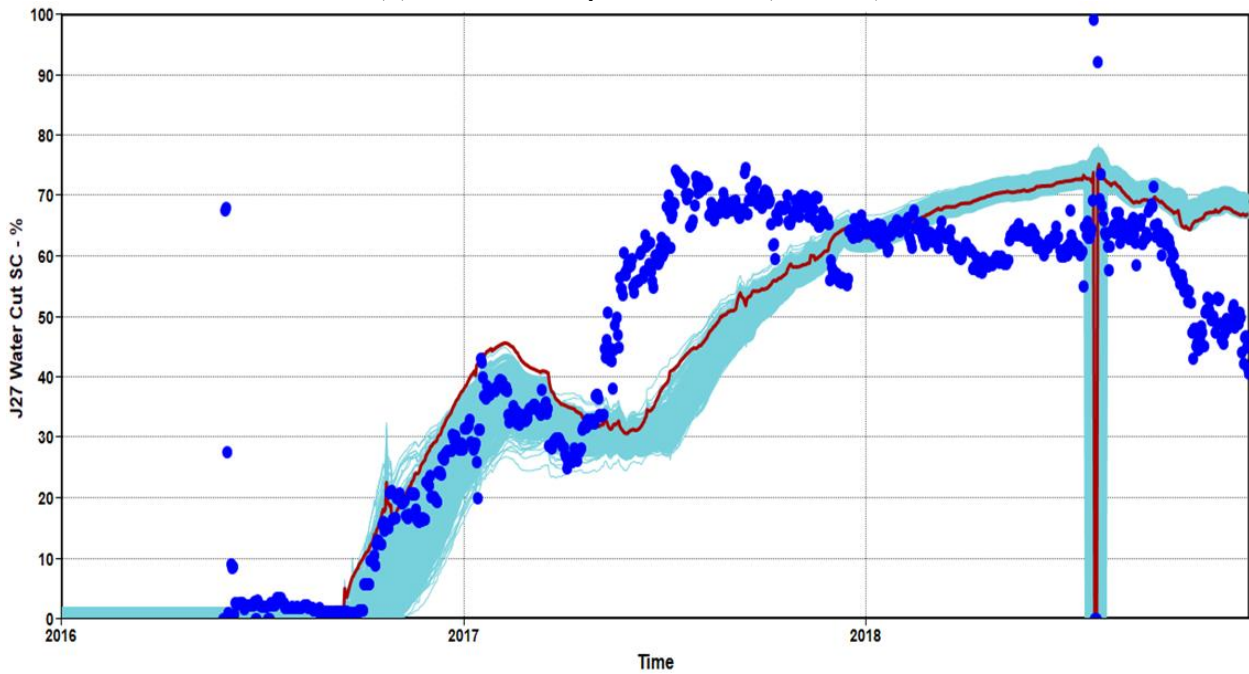
The history matching results of water cut for producer J27, as shown in **Figure 13**, are used as an example to compare the four cases.



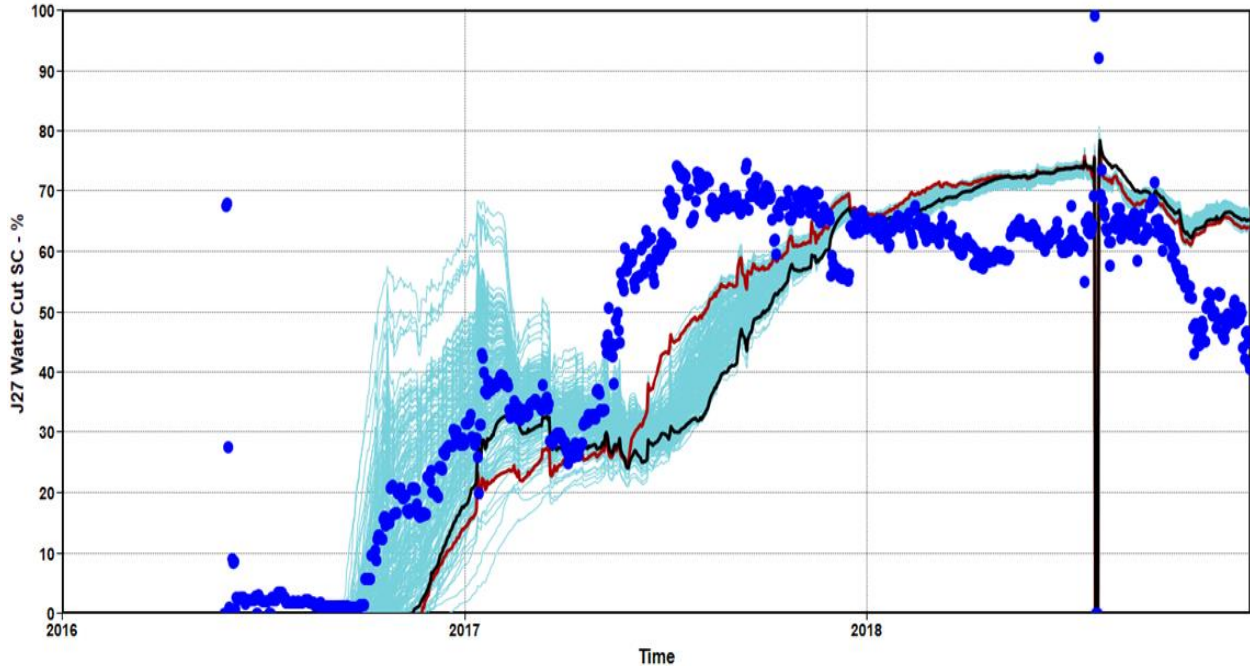
(a) Water cut of producer J27 (Case #1)



(b) Water cut of producer J27 (Case #2)



(c) Water cut of producer J27 (Case #3)



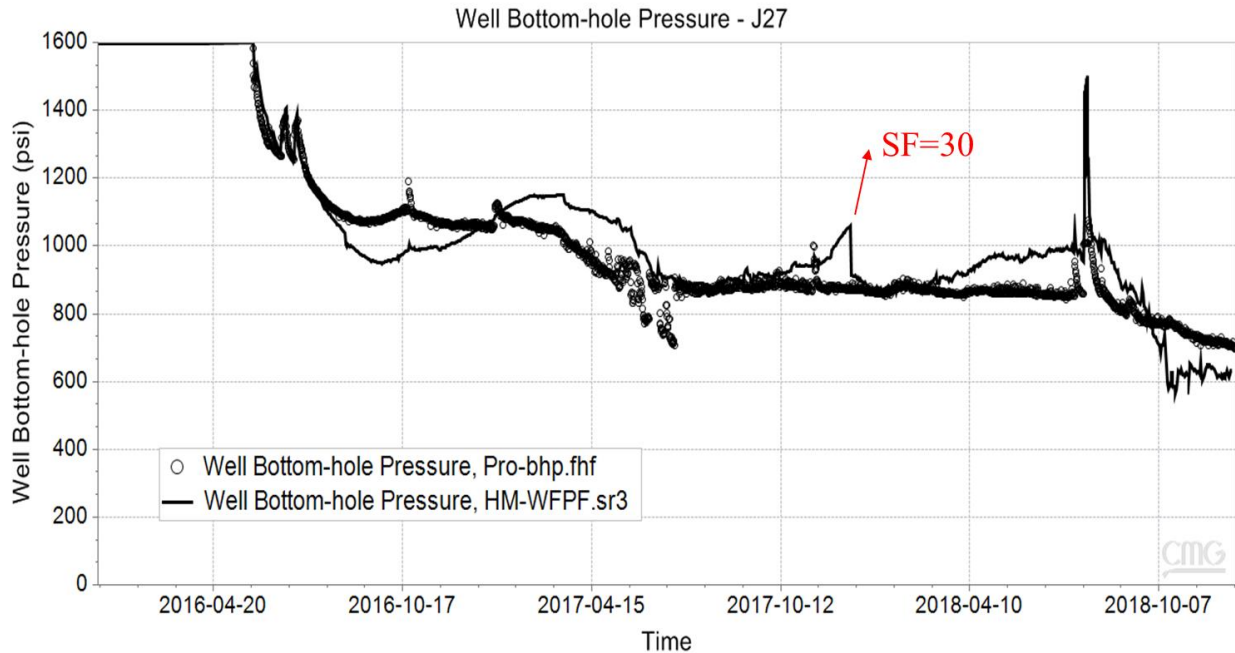
(d) Water cut of producer J27 (Case #4)

**Figure 13: History matching results of producer J27 water cut for four cases**

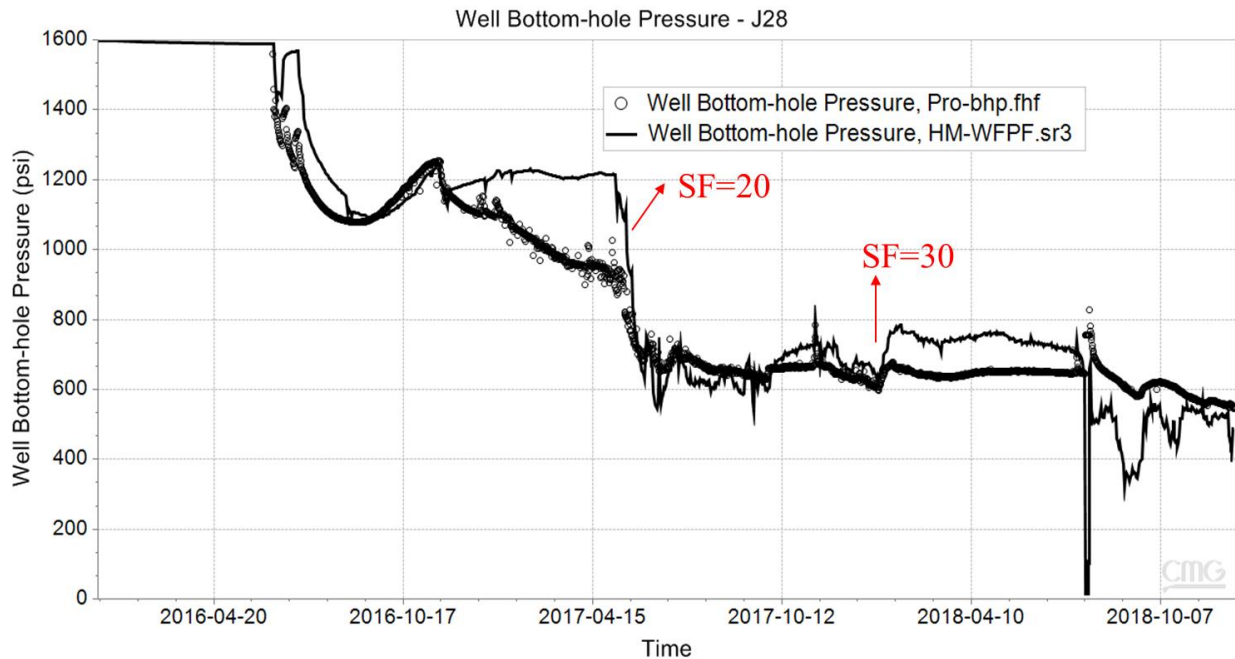
It can be found that the 8-strips simulation model yields the best history matching result. The quality of the history matching is lowered with the increasing to-be-tuned model parameters. It is because the uncertainty associated with the correlation between the production data and model parameters considerably grows when more model parameters need to be estimated by the same volume of production data. Therefore, the 8-strips model is used in future reservoir simulation.

**Relative permeability and skin factor.** Based on the history matching results of 8-strips model, the well bottom hole pressures of two production wells are matched by tuning the relative permeability and skin factors together.

The simulated well bottom hole pressures and the observed ones are compared in **Figure 14**. It indicates that the simulated well bottom hole pressures generally reproduce the trend of the observed ones. The high skin factor set in the history matching may be a reflection of sand particles migration.



(a) Well bottom hole pressure of producer J27

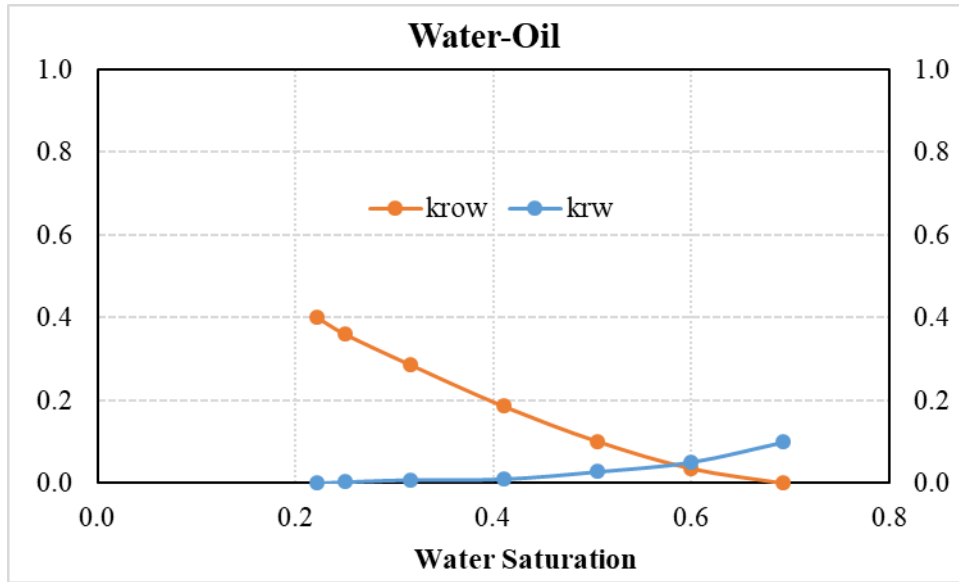


(b) Well bottom hole pressure of producer J28

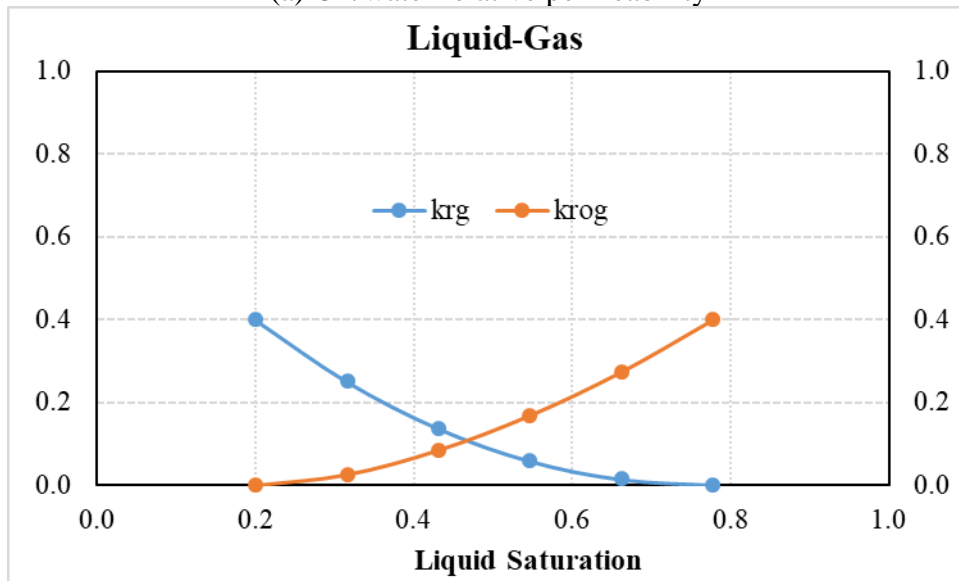
**Figure 14: History matching results of well bottom hole pressure for (a) producer J27 and (b) producer J28**

A new set of relative permeability curves obtained from the history matching is presented in **Figure 15**, which is used to characterize the fluids flow in both waterflood and polymer flood. Compared to the previous work, both the relative permeabilities of oil phase and water phase are decreased to reduce the well bottom hole pressures of two production wells in the simulation model.





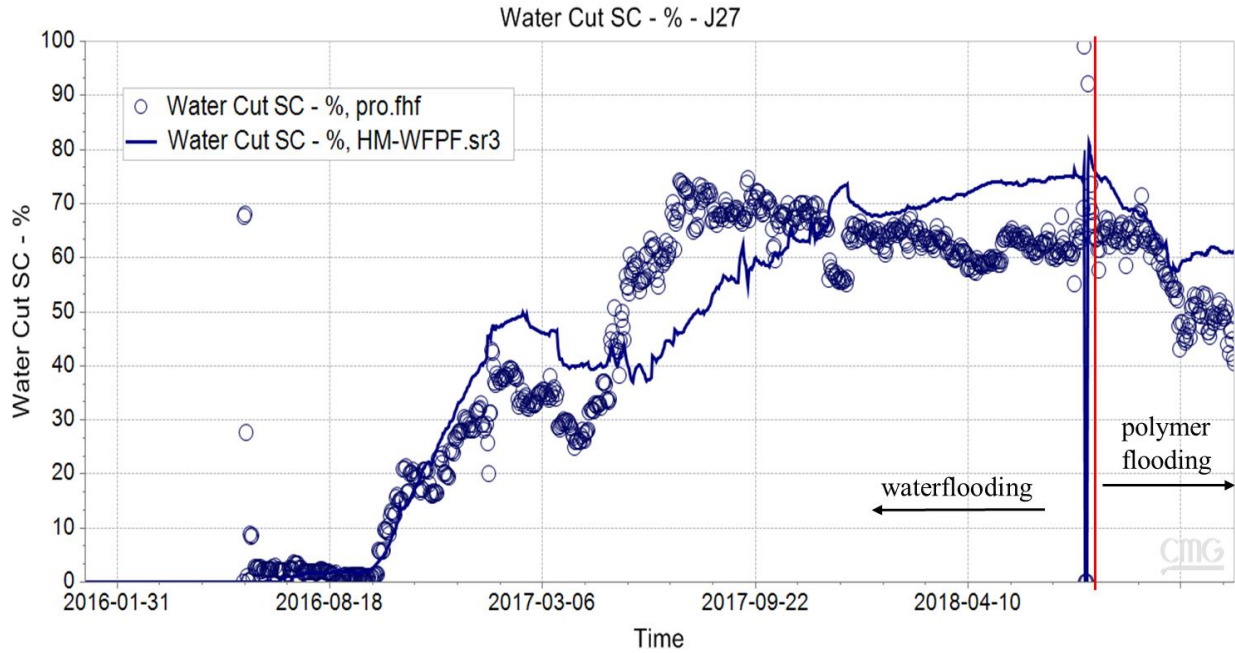
(a) Oil/water relative permeability



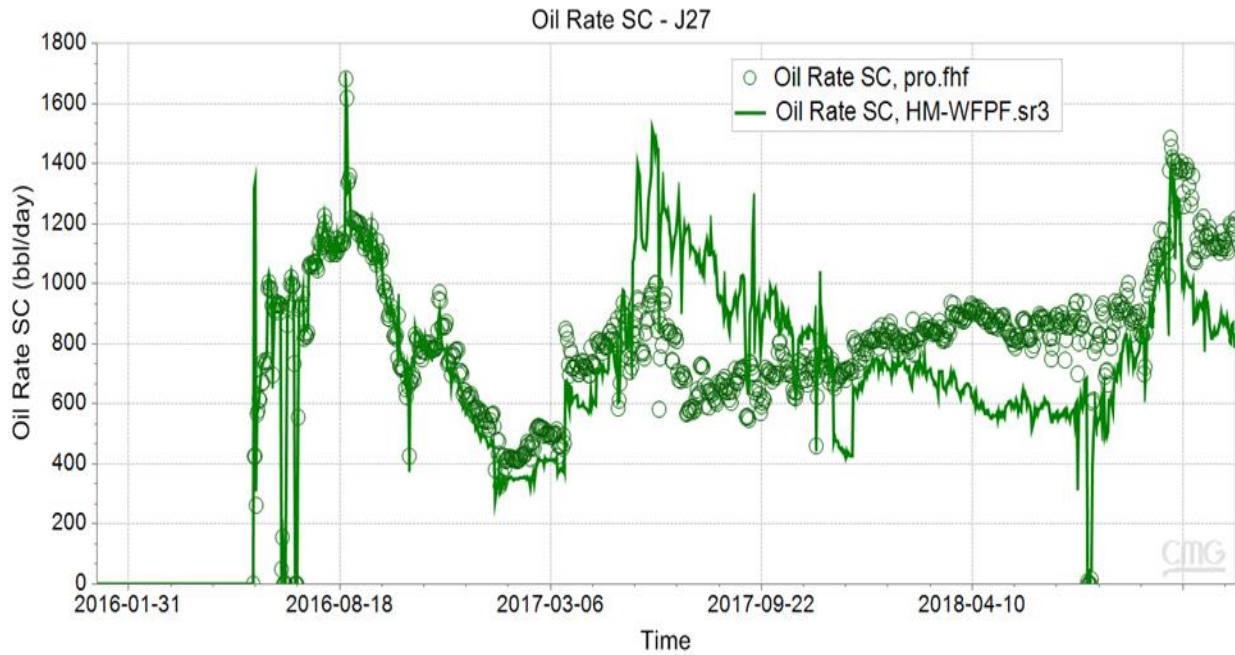
(b) Gas/oil relative permeability

**Figure 15: A new set of relative permeability curves of (a) oil/water and (b) gas/oil**

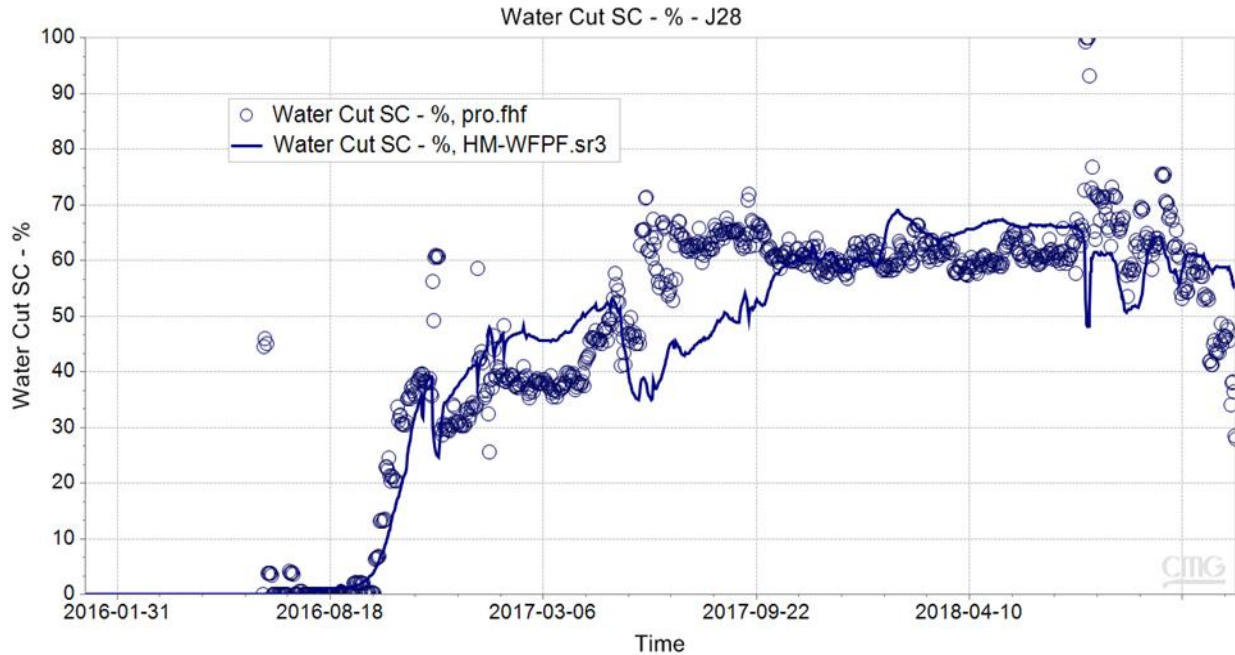
The optimal history matching results of water cut and oil production rate for two production wells are shown in **Figure 16**. It can be seen that the simulated production data agrees with the observed ones for the waterflooding period.



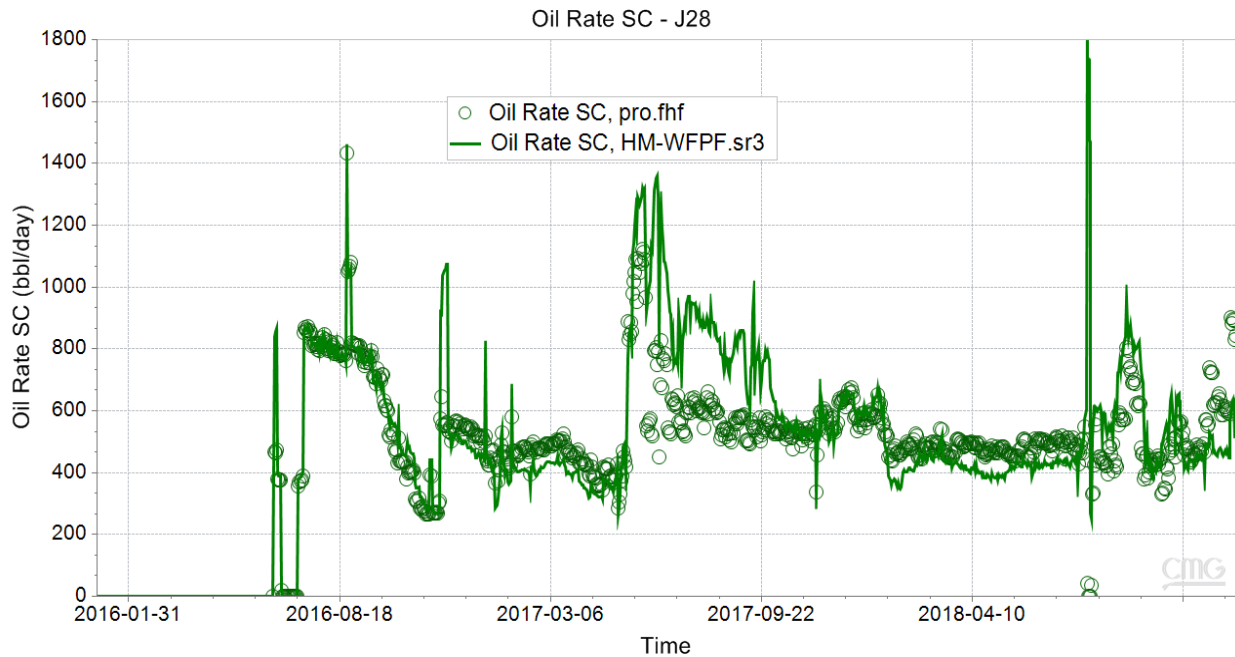
(a) Water cut of producer J27



(b) Oil production rate of producer J27



(c) Water cut of producer J28



(d) Oil production rate of producer J28

**Figure 16: History matching results of (a) water cut (b) oil production rate for producer J27 and (c) water cut (d) oil production rate for producer J28**

#### 4 Tracer test data for history matching

By collecting production data including tracer concentration from the tracer injection, the production history used to tune the reservoir simulation model was extended to March 25, 2019. The water injection rates and liquid production rates are set as well constraints in the reservoir

simulation model, while oil production rates and tracer concentration measured in producers are to be history matched using CMOST.

#### 4.1 Parameter setting of the reservoir simulation model

**Tracer parameters.** Tracer T140A and T140C, as two new components, are added to the simulation model. The properties of tracers (for example, molecular weight, critical pressure, and critical temperature) are assigned the same values as those of water. The propagation of injected tracers and chemicals employed in enhanced oil recovery (EOR) processes are influenced by the tortuous flow and heterogeneities of the porous media in which they flow. Normally, this causes the tracer to disperse at different velocities in three directions in the reservoir simulation model. Because of this, the effective total dispersion coefficients of tracer T140A and T140C in the water phase for I, J and K directions inputted in the simulation are used to specify the flowability of tracers in the reservoir. Initially, the total dispersion coefficients of T140A in I, J and K directions are assigned to be  $1 \times 10^{-8}$ ,  $1 \times 10^{-4}$  and  $1 \times 10^{-8}$ , respectively, while the total dispersion coefficients of T140C in I, J and K directions are assigned to be  $1 \times 10^{-4}$ ,  $1 \times 10^{-2}$  and  $1 \times 10^{-4}$ , respectively. The mole fraction of tracer in the injection fluid is calculated by using the mass of the injected tracer and the injected water. In the simulation model, the mole fraction of T140A in injector J24A is  $6 \times 10^{-4}$ , and the mole fraction of T140C in injector J23A is  $4 \times 10^{-4}$ .

**Permeability heterogeneity.** Tracer test data shows that T140C was first observed in J27 on October 12, 70 days after injection, and the tracer concentration reached a peak at 155 days. It indicates there may exist strong communication between injector J23A and producer J27. Therefore, a block/strip permeability field is developed, as shown in **Figure 17**, to identify the potential high permeable channels between injector J23A and producer J27.

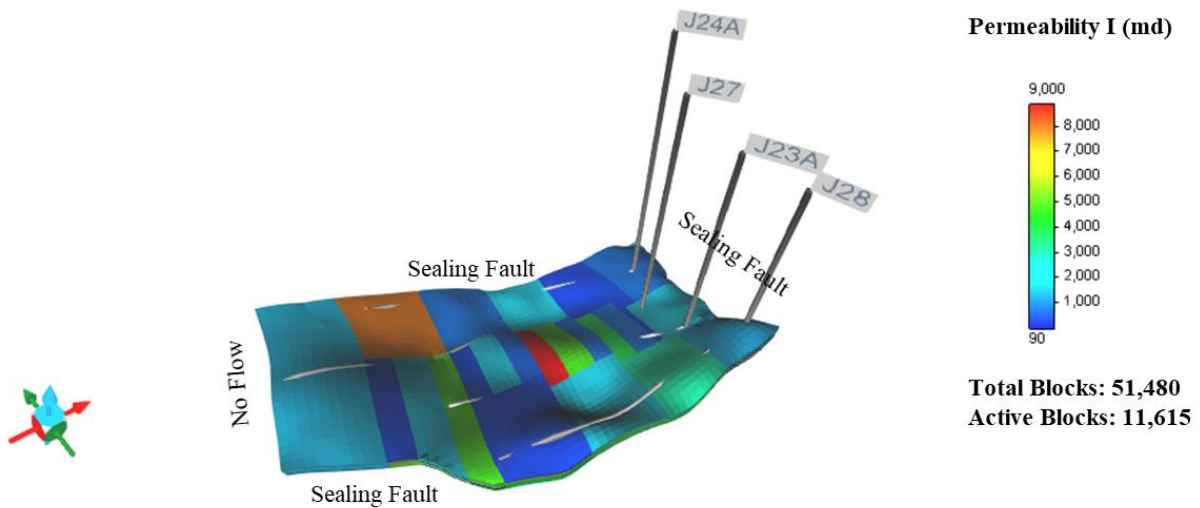


**Figure 17: Permeability heterogeneity of block/strip type in the simulation model**

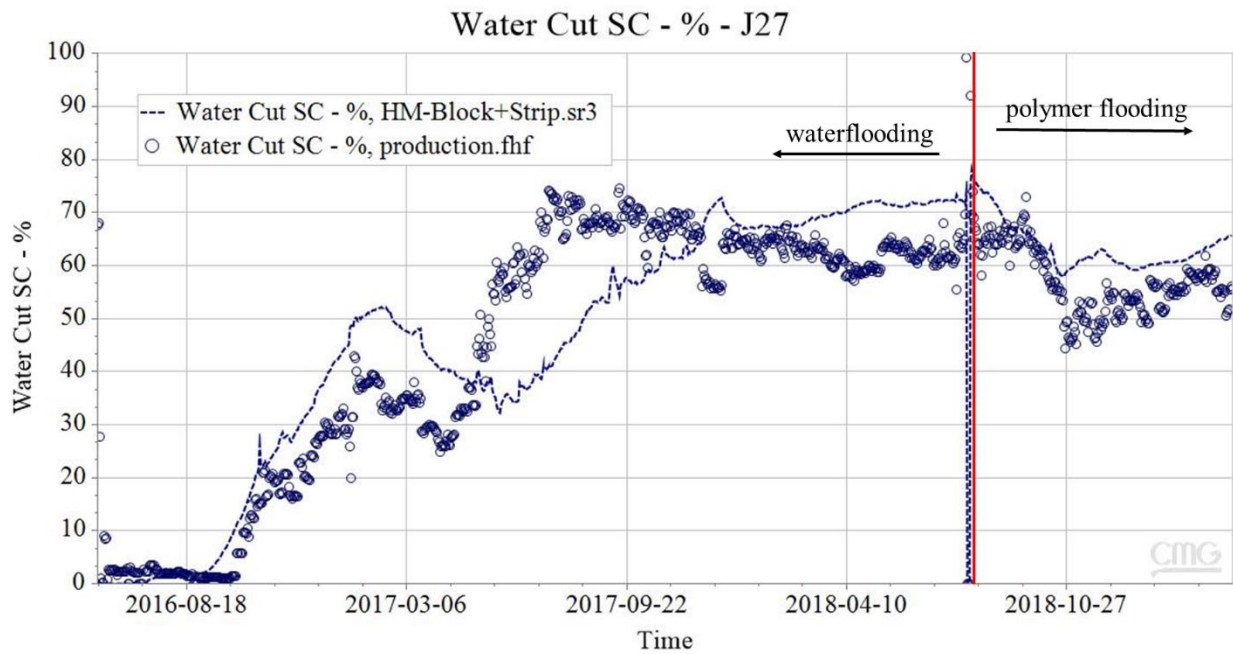
Twenty-six permeability blocks/strips are assigned in each layer, resulting in 130 permeability blocks/strips in the whole reservoir simulation model. The permeability of the blocks/strips in each layer are initially assigned with the average permeability of the layer (layer 1: 1806 mD, layer 2: 1598 mD, layer 3: 2269 mD, layer 4: 1801 mD and layer 5: 1029 mD) and then tuned between 100 and 7600 mD during the history matching process. In addition, the average porosity of each layer

(layer 1: 0.3476, layer 2: 0.3474, layer 3: 0.3537, layer 4: 0.3497 and layer 5: 0.3417) and the estimated relative permeability curves, as shown in **Figure 15**, from the previous history matching results are used in the simulation model.

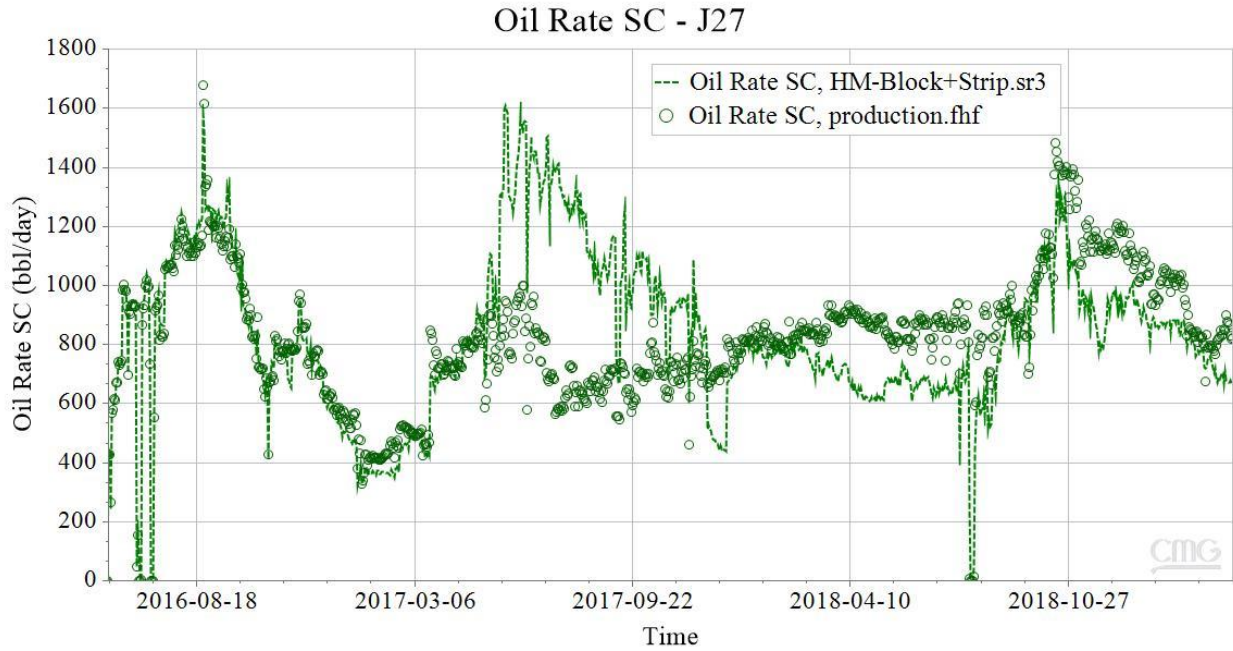
#### 4.2 History matching results

During the history matching, we try to match not only the production profiles of waterflooding and polymer flooding but also the concentration profiles of tracer T140A and T140C in two producers. Tracer test data unit in part per billion (ppb) is converted to water mass fraction used in the simulation model. The permeability of the blocks/strips in five layers and the total dispersion coefficients of tracer T140A and T140C are tuned together to try to match the water cut and water mass fraction of T140A and T140C in CMOST.

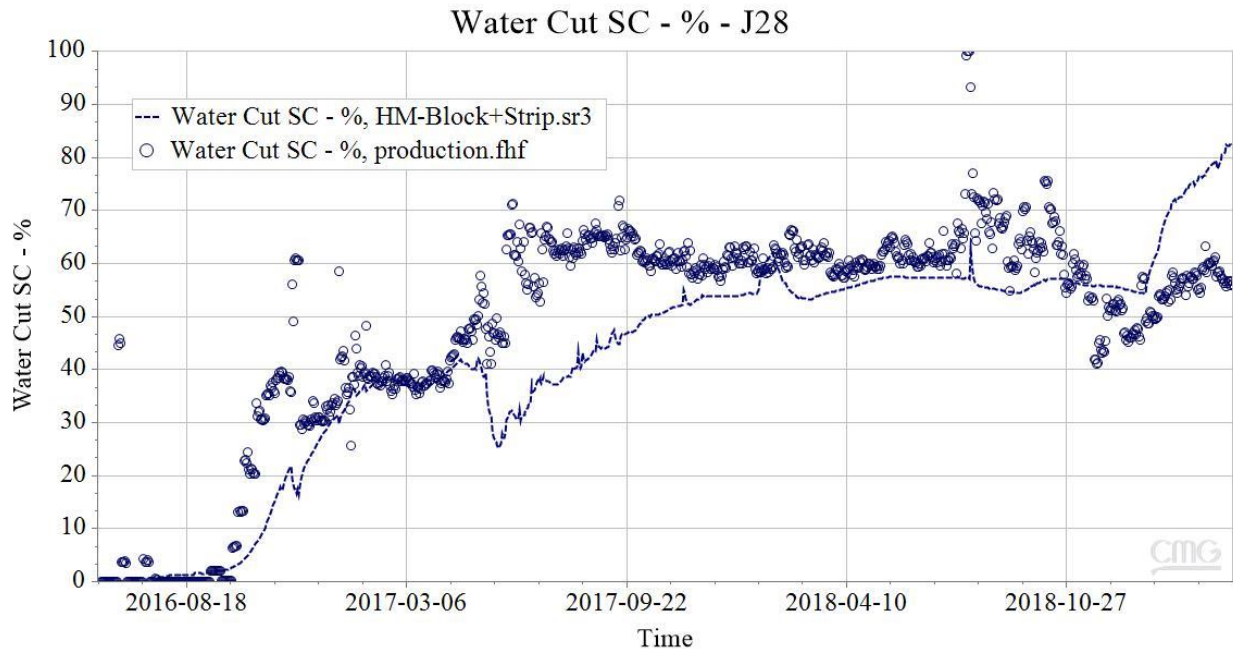
The optimal history matching results of water cut and oil production rate for two production wells are shown in **Figure 18**. It can be seen that the simulated production data are close to the observed ones for the polymer flooding period. As for the waterflooding period, the history matching results are not better than the previous work.



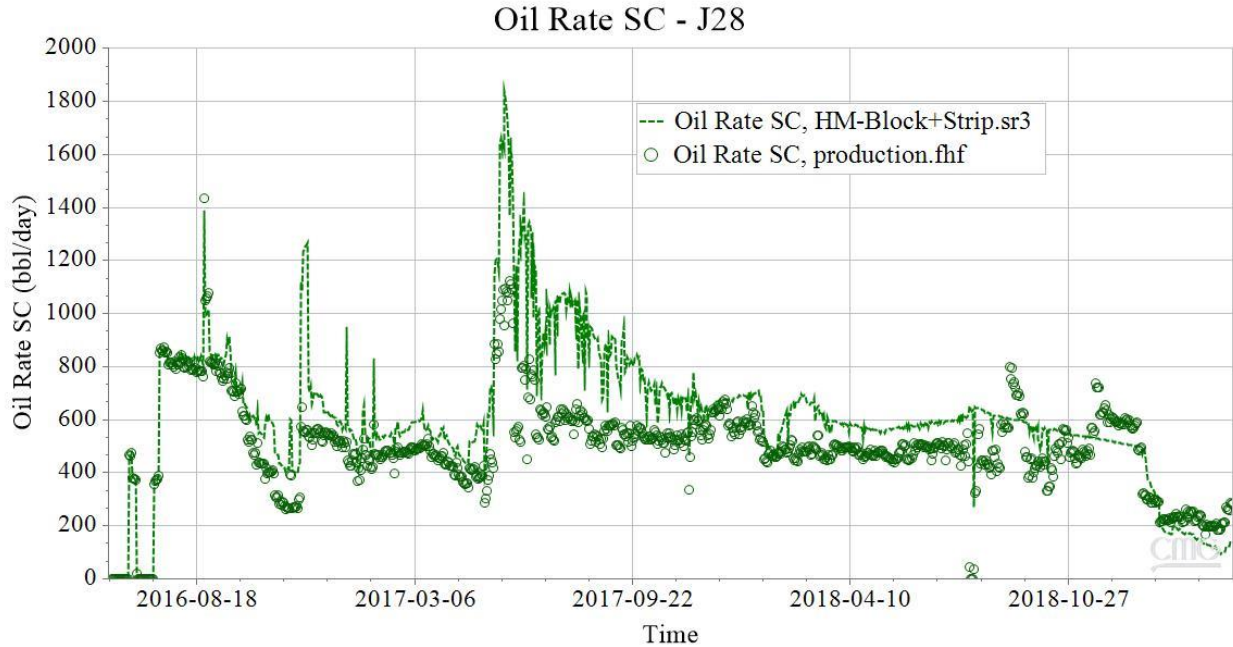
(a) Water cut of producer J27



(b) Oil production rate of producer J27



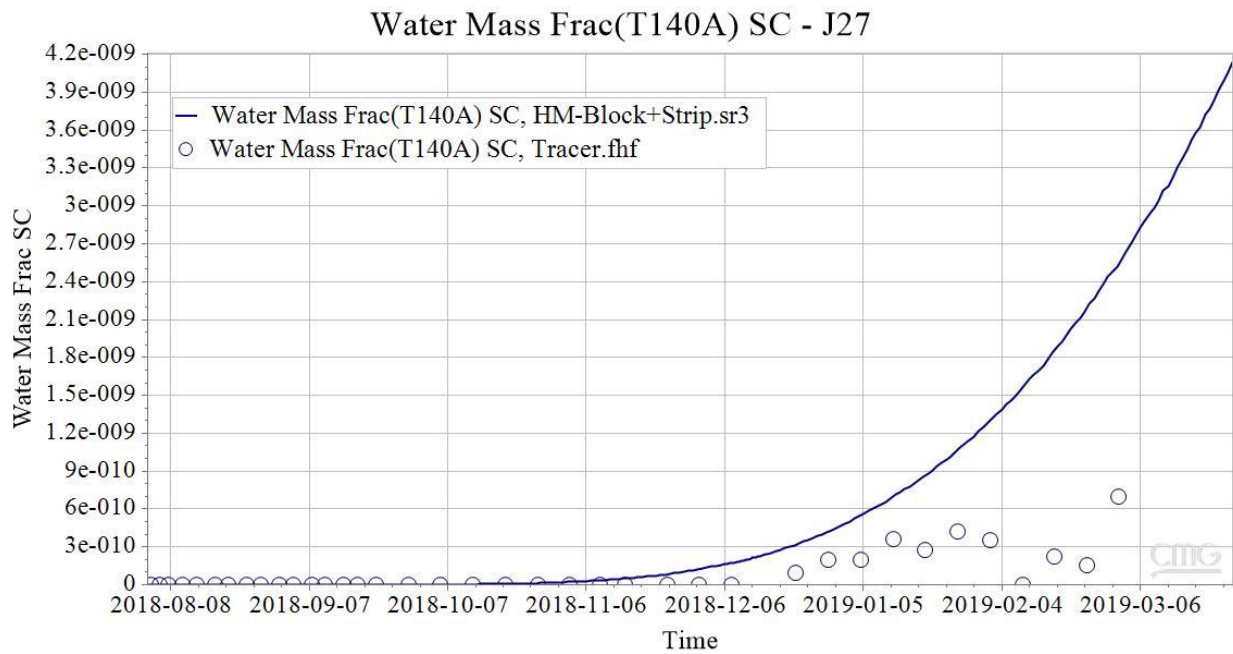
(c) Water cut of producer J28



(d) Oil production rate of producer J28

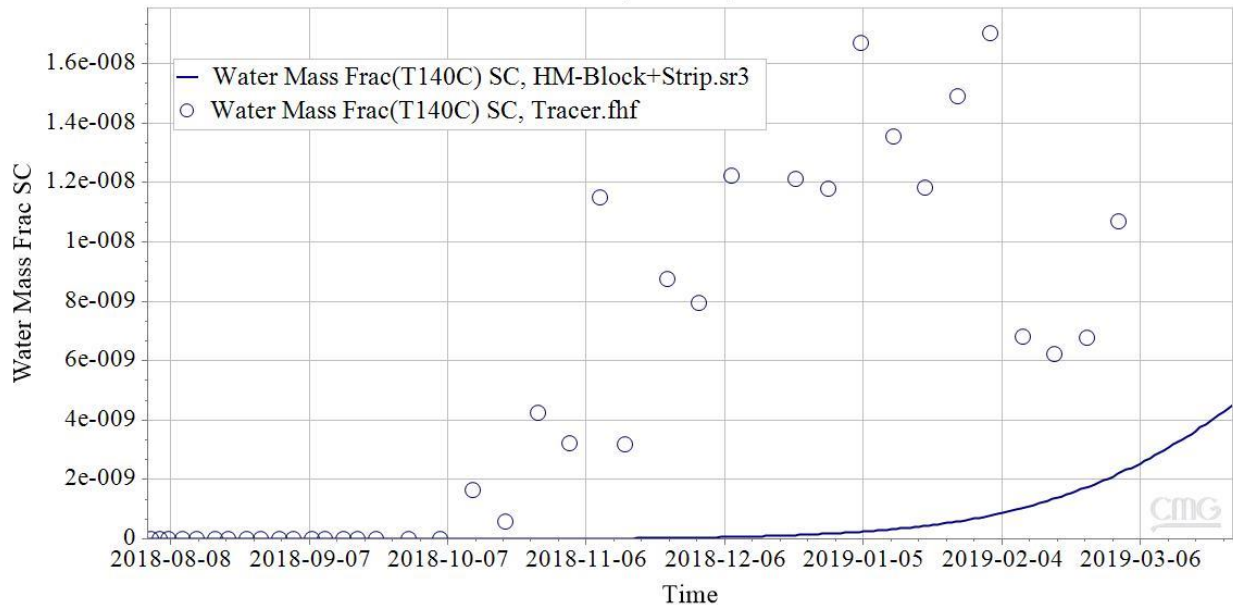
**Figure 18: History matching results of (a) water cut (b) oil production rate for producer J27 and (c) water cut (d) oil production rate for producer J28**

The history matching results of tracer concentration in producer J27 and J28 is presented in **Figure 19**. It can be seen that there is an agreement between observed data and updated simulation result of T140C concentration in producer J28. Although tracer concentration profiles in producer J27 obtained from the updated simulation model can reflect the increasing trends of concentration, there still exist significant disagreement between the simulated data and observed data.



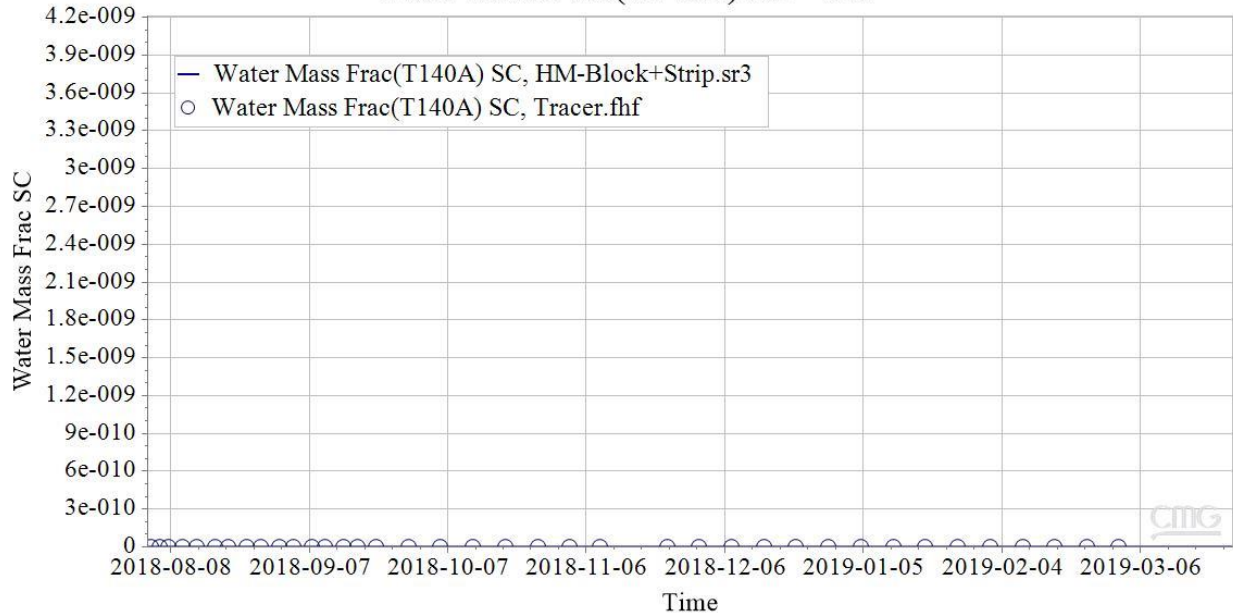
(a) History matching results of T140A in producer J27

Water Mass Frac(T140C) SC - J27



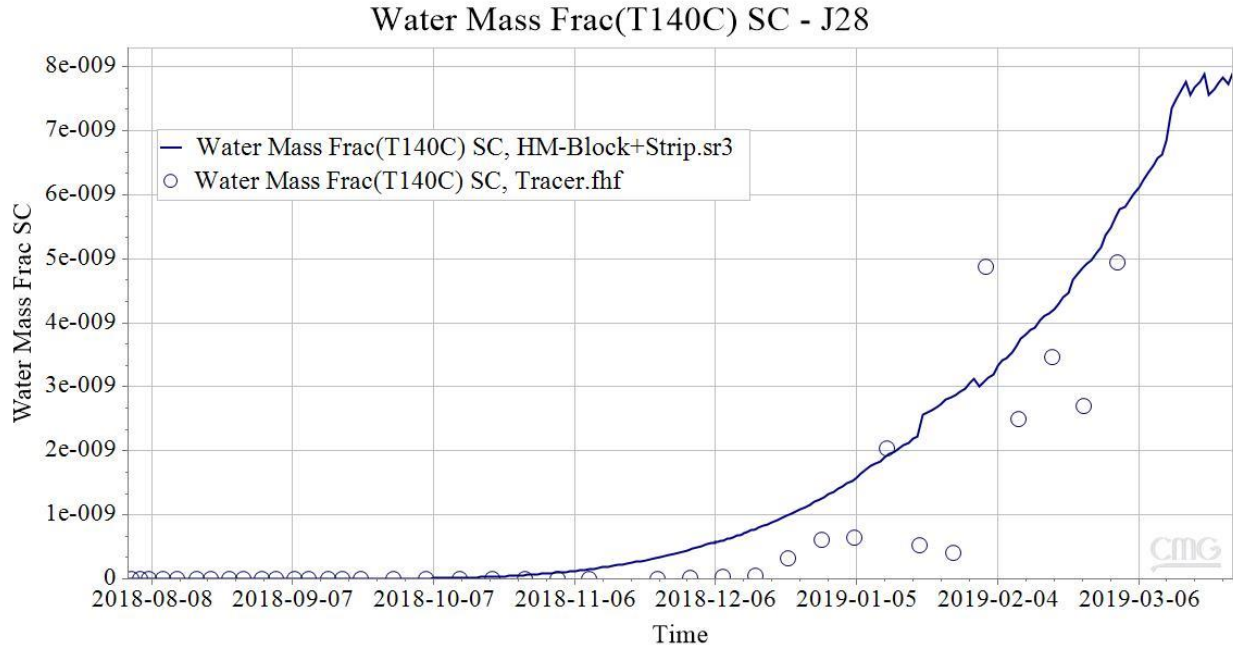
(b) History matching results of T140C in producer J27

Water Mass Frac(T140A) SC - J28



(c) History matching results of T140A in producer J28





(d) History matching results of T140C in producer J28

**Figure 19: History matching results of (a) T140A concentration (b) T140C concentration in producer J27 and (c) T140A concentration (d) T140C concentration in producer J28**

### 4.3 Updated reservoir simulation model

After history matching, the updated block/strip type permeability heterogeneity of the reservoir simulation model is presented in **Figure 20**. Meanwhile, the total dispersion coefficients of T140A in I, J and K directions are  $3.52 \times 10^{-7}$ ,  $8.24 \times 10^{-5}$  and  $3.63 \times 10^{-10}$ , respectively, and the total dispersion coefficients of T140C in I, J and K directions are  $9.51 \times 10^{-9}$ ,  $2.70 \times 10^{-4}$  and  $1.82 \times 10^{-5}$ , respectively.

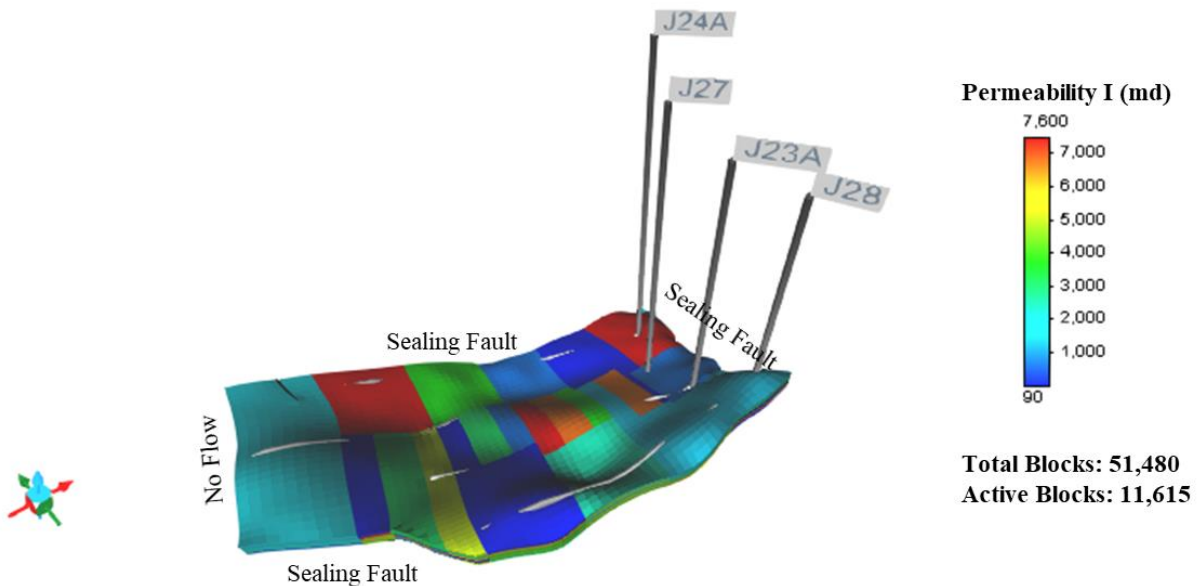


**Figure 20: Updated permeability heterogeneity of the reservoir simulation model**

## 5 Reservoir EOR performance prediction

The updated simulation model, as shown in **Figure 20**, is used to forecast the production performance of the waterflooding and polymer flooding, respectively, for 10 years from March 25, 2019. During the prediction periods, the water injection rates of J23A and J24A are constrained to be 2400 bbl/day and 1200 bbl/day, respectively. Also, to honor the material balance, the liquid production rates of J27 and J28 are constrained to be 2400 bbl/day and 1200 bbl/day, respectively. The following six case studies are conducted to investigate the reservoir EOR performance:

Case #1: inject water for 10 years

Case #2: inject polymer for 2 years followed by 8 years of waterflooding

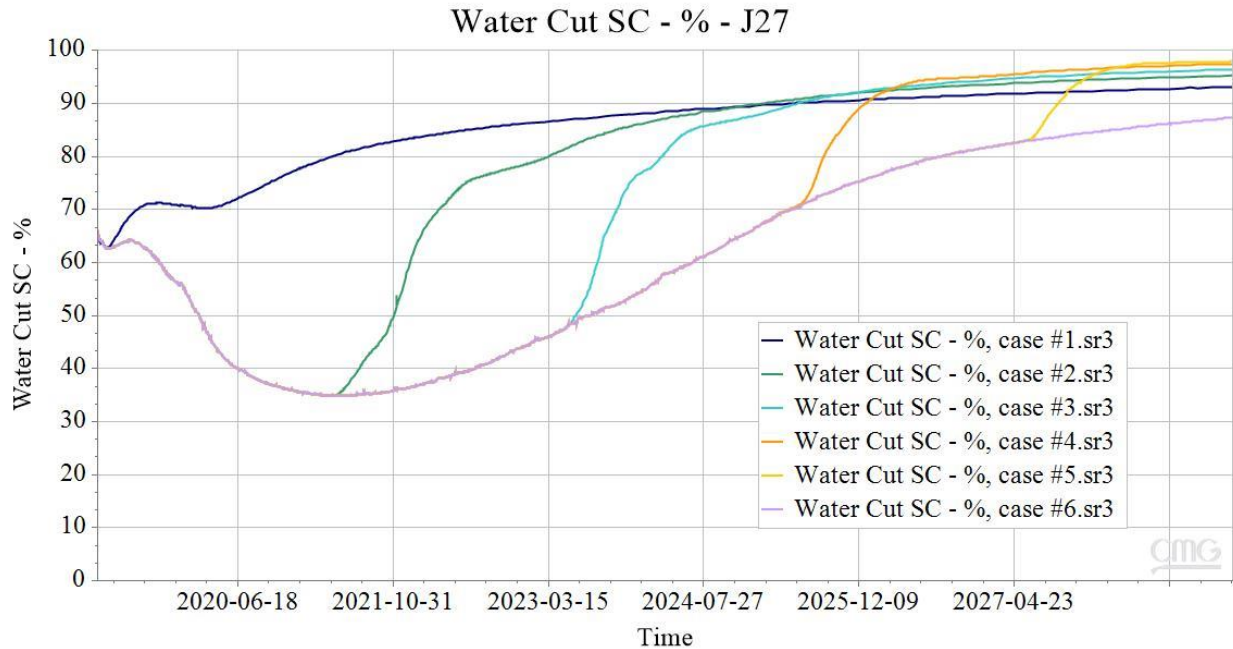
Case #3: inject polymer for 4 years followed by 6 years of waterflooding

Case #4: inject polymer for 6 years followed by 4 years of waterflooding

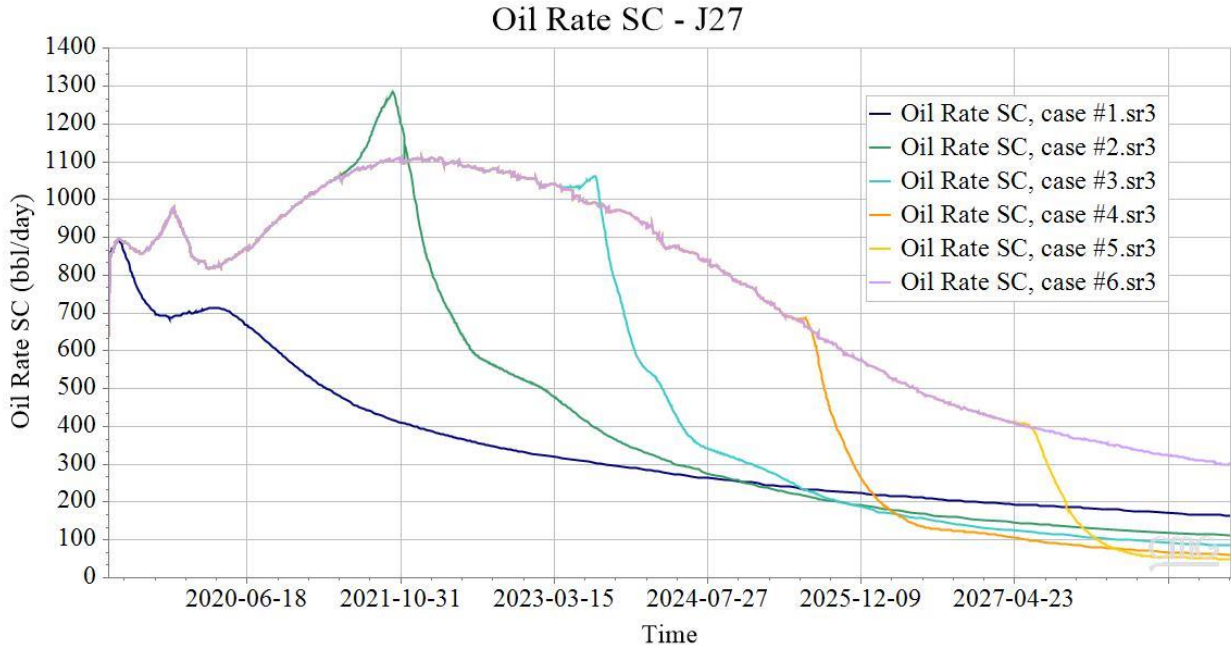
Case #5: inject polymer for 8 years followed by 2 years of waterflooding

Case #6: inject polymer for 10 years

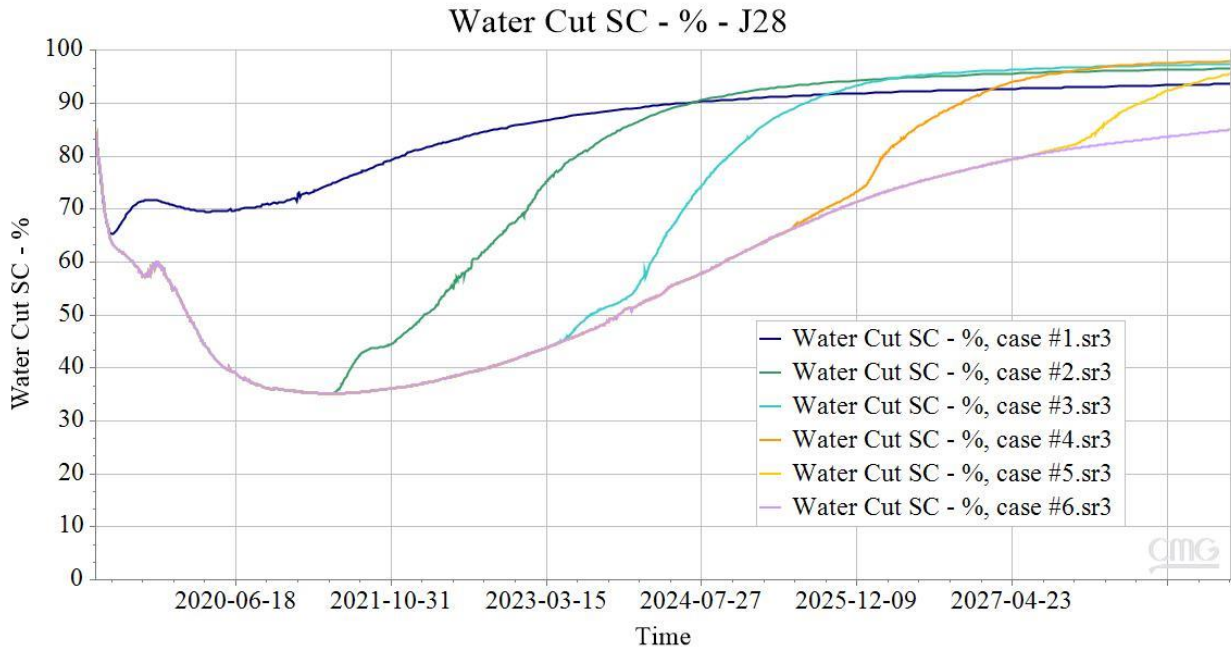
The predicted production profiles of the water cut and oil production rate for two producers are presented in **Figure 21**.



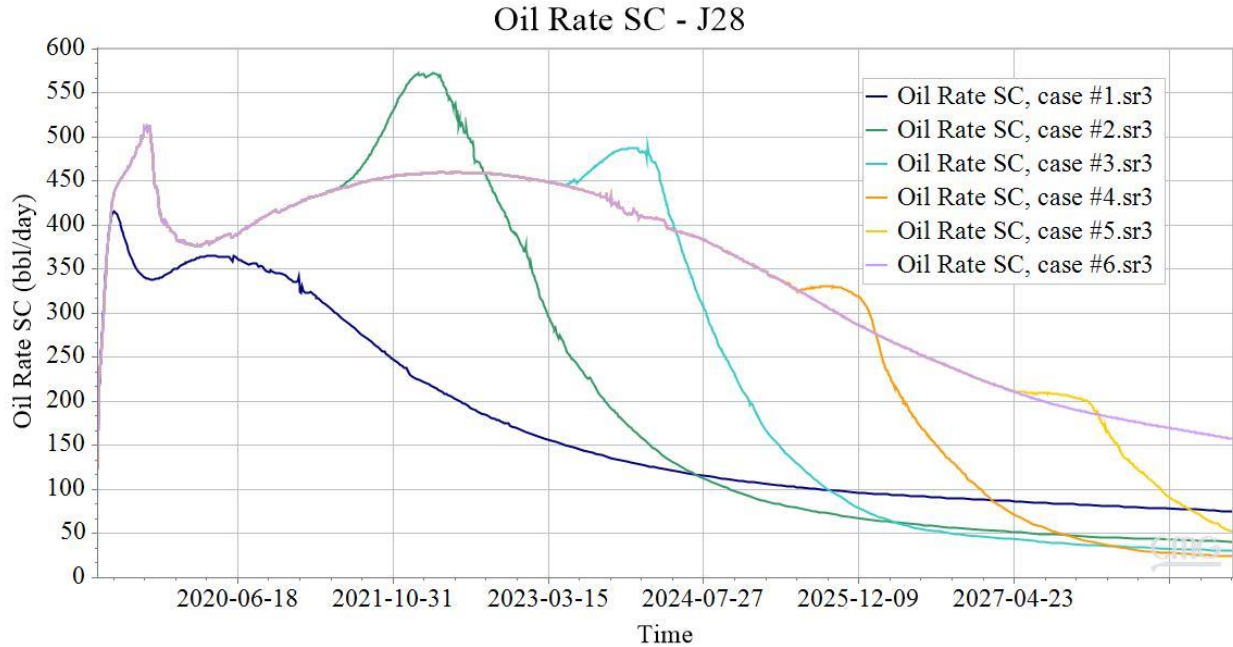
(a) Water cut of producer J27



(b) Oil production rate of producer J27



(c) Water cut of producer J28



(d) Oil production rate of producer J28

**Figure 21: Predicted production profiles of (a) water cut (b) oil production rate in producer J27 and (c) water cut (d) oil production rate in producer J28**

As can be seen, the water cuts will decrease to a minimum in March 2021 and can be reduced by up to 40% using polymer flooding compared to waterflooding. After injecting polymer, the oil production rates will reach a peak and then drop to less than those of waterflooding in two years.

The oil recovery factor for each case during the prediction periods are shown in **Figure 22**. The oil recovery factor can merely reach 25% by the waterflooding in 10 years, but it will be promoted significantly by injecting polymer. More oil can be produced by increasing the amount of injected polymer, and the oil recovery factor will increase to 41% if the polymer is injected continuously for the next 10 years.

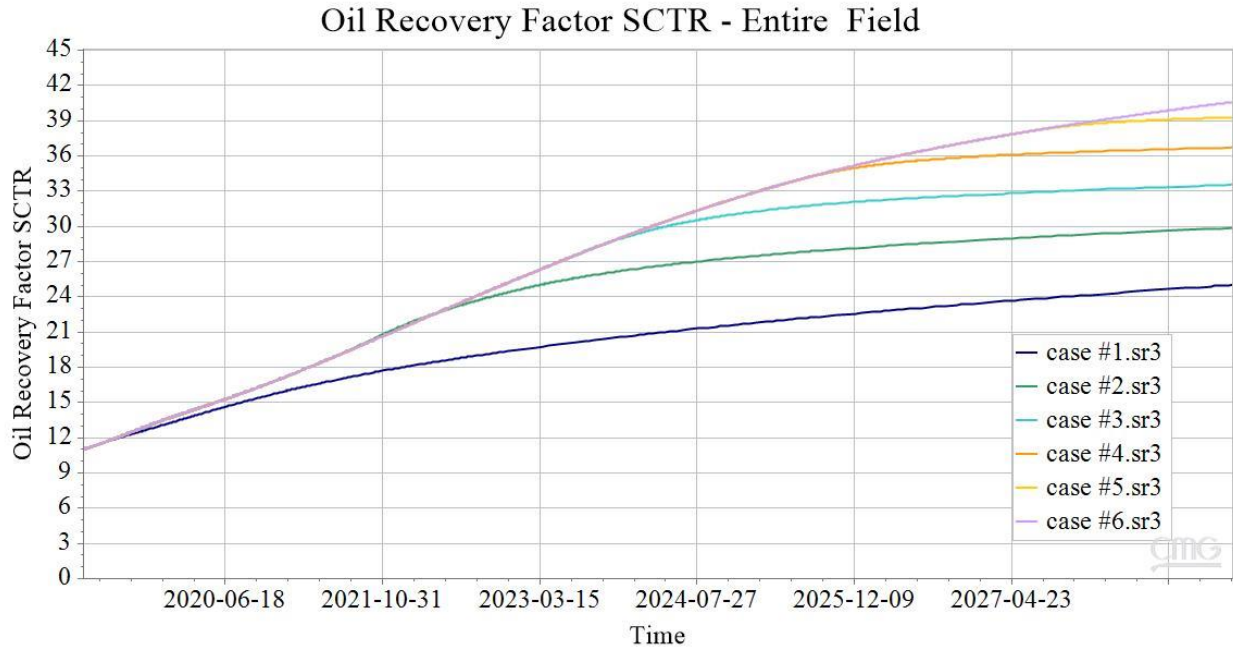


**Figure 22: The profiles of oil recovery factor of the entire field by injecting different amounts of polymer in the next 10 years**

## 6 Conclusions

- (1) A field-scale reservoir simulation model has been built by using the geological and reservoir data provided by Hilcorp, and history matching has been conducted to validate the built reservoir model. Finally, waterflooding and polymer flooding performance have been predicted, respectively, using the validated reservoir model, and their performances have been compared.
- (2) The humps on the water cut curves can be well produced in the simulation using the heterogeneous and strip type permeability distribution instead of using the homogeneous permeability in a layer cake model.
- (3) The simulated and actual water cut curves for two production wells can achieve a good agreement by tuning the relative permeability curves which are parameterized by using the power-law model. The estimated relative permeability curves are able to capture the multiphase flow performance in the waterflooding process.
- (4) The 8-strips permeability model yields the best history matching results among 8-strips, 16-strips, 32-strips and 16-blocks permeability models. The quality of history matching is lowered with the increasing to-be-tuned model parameters.
- (5) The simulated well bottom hole pressure generally reproduce the trend of the observed ones by tuning the relative permeability and skin factor based on the history matching results of 8-strips permeability model.
- (6) The simulated production data are close to the observed ones in the polymer flooding process by history matching oil production rate and tracer concentration in a block/strip permeability model.
- (7) The oil recovery factor can be promoted significantly by injecting polymer compared to the waterflooding in 10 years, and the water cuts will be reduced by up to 40% using polymer flooding.

## **7 Future work**

UAF's future work will focus on updating the reservoir model by matching cumulative oil production using tracer test data. And then the history matching results obtained from matching different production data will be compared.